

A
Dissertation Report
On
**CFD based Thermal Performance Analysis of Earth Air
Tunnel Heat Exchanger System with Water Impregnation**

Submitted By

ANKIT GOYAL
(2015PTE5245)

Under the Supervision of

Dr. G. D. AGRAWAL
Associate Professor
Department of Mechanical Engineering
MNIT, Jaipur India

Submitted in Partial Fulfilment of the Requirements for the Award of Degree of

Master of Technology
In
Thermal Engineering



DEPARTMENT OF MECHANICAL ENGINEERING
MALAVIYA NATIONAL INSTITUTE OF TECHNOLOGY, JAIPUR

2017



**DEPARTMENT OF MECHANICAL ENGINEERING
MALAVIYA NATIONAL INSTITUTE OF TECHNOLOGY
JAIPUR (RAJASTHAN)-302017**

CERTIFICATE

This is to certify that the dissertation entitled “**CFD based Thermal Performance Analysis of Earth Air Tunnel Heat Exchanger(EATHE) System with Water Impregnation**” which is being submitted by *Mr. Ankit Goyal (ID No.2015 PTE 5245)* in partial fulfilment of the award of the degree of **Master of Technology in Thermal Engineering** of Malaviya Institute of Technology, Jaipur is found to be satisfactory and is hereby approved for submission.

Date:

Place:

Dr. G. D. Agrawal

Associate Professor

Dept. of Mechanical Engg.

MNIT, Jaipur, India



**DEPARTMENT OF MECHANICAL ENGINEERING
MALAVIYA NATIONAL INSTITUTE OF TECHNOLOGY
JAIPUR (RAJASTHAN)-302017**

DECLARATION

I **Ankit Goyal** hereby declare that the dissertation entitled “ **CFD based Thermal Performance Analysis of Earth Air Tunnel Heat Exchanger(EATHE) System With Water Impregnation**” being submitted by me in partial fulfilment of the degree of **M. Tech (Thermal Engineering)** is a research work carried out by me under the supervision of **Dr. G. D. Agrawal** and the contents of this dissertation work, in full or in parts, have not been submitted to any other Institute or University for the award of any degree or diploma. I also certify that no part of this dissertation work has been copied or borrowed from anyone else. In case any type of plagiarism is found out, I will be solely and completely responsible for it.

Date:

Ankit Goyal

Place:

M.Tech. (Thermal Engg.)
2015PTE5245

ACKNOWLEDGEMENT

I feel immense pleasure in conveying my heartiest thanks and profound gratitude to my supervisor **Dr. G. D. Agrawal**, who provided me with his generous guidance, valuable help and endless encouragement by taking personal interest and attention. No words can fully convey my feelings of respect and regard for him.

I would like to express my sincere and profound gratitude to **Mr. Sheetal Kumar Jain, Mr. Kamal Agrawal** (Research Scholar), **Dr. Anuj Mathur, Mr. Mitesh Varshney and Mr C.P Chandra Sekhar** Mechanical Engineering Department, Malaviya National Institute of Technology, Jaipur, who were abundantly helpful and offered invaluable assistance, support and guidance with their experience and knowledge, throughout my dissertation work. I feel greatly indebted for teaching me the concepts of ANSYS and FLUENT, without which it would have been very difficult to move ahead with my work.

I also express my deepest gratitude to my **parents** and my **brother** for their blessings and affection, without which I would not be able to endure hard time and carry on. Last but not the least; I am grateful to Almighty God, without whom blessings I could not have achieved so much.

(Ankit Goyal)

ABSTRACT

Geothermal energy is one of the renewable energy sources that people have an easy access to for supplying low grade thermal energy with a low impact on the environment. The methods of utilizing geothermal energy for buildings include ground source heat pumps and earth to air heat air exchangers. EATHE system has often been used to achieve free cooling/heating for energy saving. EATHE is an underground heat exchanger that works through burying pipes in the ground, which can cool or warm air by dissipating heat to or capturing heat from the ground. In a typical Earth to Air Heat Exchanger (EAHE) system hot/cold outdoor air during summer/winter is passed through the grounded buried pipes. When air flows through the pipes, heat is exchanged to/from the soil. As a result, temperature of air at the outlet of EATHE is much higher/lower than that of the ambient air. During summer, the outlet air coming from EAHE can be directly used for space cooling if its temperature is low enough after heat exchanging process. The effectiveness and performance of EATHE system can also be increased by increasing soil moisture content, making wet configuration of system. Both above configurations of EAHE can contribute to the reduction in energy consumption for space conditioning. In second configuration effectiveness and performance of EATHE is enhanced. The EAHE system is also called EATHE (earth air tunnel heat exchanger).

In this study, commercial CFD software ANSYS FLUENT (ver. 15.0.7) is used to develop and simulate the EATHE system to compare and validate its results with the secondary experimental study. The geometrical model has been created for simple(dry) tunnel having pipe length 68.9 m length and diameter 0.01m while the soil volume created as concentric cylinder over the pipe having length 65.2 m and diameter 0.1m. One end of the pipe is the inlet of air while the other end of the pipe is the outlet. In the experimental part, outlet is insulated hence no heat transfer is consider in the outlet. To keep the same working condition in simulation study, we removed the soil from pipe in the outlet part.

This study consists of development of four different models of EATHE system i.e. dry soil system, soil with 5% moisture content, soil with 10% moisture content and soil with 15% moisture content. We simulated the model for three different time intervals i.e. 1 hour, 6 hours and 11 hours operation for each case and compare the results with

the experimental study. Results shows that knee length of dry soil for 1 hour, 6 hours and 11 hours of operation comes out to be 41m, 42m and 45m respectively. Wet soil of 5% moisture content having soil thermal conductivity 0.74 W/m-K, knee length for 1 hour, 6 hours and 11 hours of operation comes out to be 30 m, 34 m and 40 m respectively. Wet soil of 10% moisture content having soil thermal conductivity 0.917 W/m-K, knee length for 1 hour, 6 hours and 11 hours of operation comes out to be 22 m, 25 m and 27 m respectively. Wet soil of 15% moisture content having soil thermal conductivity 1.22 W/m-K, knee length for 1 hour, 6 hours and 11 hours of operation comes out to be 20 m, 21 m and 23 m respectively. Velocity variation of dry soil for one hour operation were also studied. Three different velocity i.e. 2m/s, 4m/s and 6m/s was simulated. It was observed from the results that as we keep on increasing the velocity of incoming air the heat transfer rate keep on decreasing and incoming air will needed longer pipe to cool. Hence greater the velocity of incoming air, farther the knee length.

TABLE OF CONTENTS

	Page No.
Certificate	i
Declaration	ii
Acknowledgement	iii
Abstract	iv
Table of Contents	vii
List of Figures	ix
List of Tables	xi
Nomenclature	xiv
List of Abbreviations	xv
1. INTRODUCTION	1
1.1 Background of EATHE system	1
1.2 Passive Cooling Techniques	2
1.3 Principle of EATHE system	3
1.4 EATHE system with wet soil	5
1.5 Objectives of the present research	5
1.6 Scope of present research	5
1.7 Thesis Organization	6
2. LITERATURE REVIEW	7
2.1 Numerical or mathematical modeling	7
2.2 Experimental investigations	9

2.3	Modeling using computer simulations	13
2.4	Summary of literature review	15
3.	SYSTEM DESCRIPTION AND SIMULATION SETUP	17
3.1	Physical model	17
3.2	Simulation model	18
3.2.1	Governing Equations	18
3.2.2	Boundary and initial condition	19
3.2.3	Convergence and grid independence test	19
3.3	Model validations	21
3.3.1	Introduction to existing experimentally facility	21
3.3.2	Comparison between experimental and simulation model for validation	21
4	PERFORMANCE ANALYSIS OF DRY AND WET EATHE SYSTEMS	
4.1	Geometric modelling	24
4.2	Modelling	24
4.3	Numerical solution and setup	24
4.3.1	Numerical solver used	25
4.3.2	Solution Technique	26
4.3.3	Turbulence Model	27
4.3.4	Convergence criteria	30
4.3.5	Input parameters	30
4.3.6	Grid independence test	32

5 RESULTS AND DISCUSSION

5.1	Performance analysis of dry EATHE systems for summer cooling	34
5.1.1	Results of dry soil simulation of 1 hour operation	34
5.1.2	Results of dry soil simulation of 6 hours operation	35
5.1.3	Results of dry soil simulation of 11 hours operation	36
5.2	Performance analysis of wet EATHE systems with 5% moisture content for summer cooling	36
5.2.1	Results of soil with 5% moisture content simulation of 1 hour operation	36
5.2.2	Results of soil with 5% moisture content simulation of 6 hours operation	37
5.2.3	Results of soil with 5% moisture content simulation of 11 hours operation	38
5.3	Performance analysis of wet EATHE systems with 10% moisture content for summer cooling	38
5.3.1	Results of soil with 10% moisture content simulation of 1 hour operation	38
5.3.2	Results of soil with 10% moisture content simulation of 6 hours operation	39
5.3.3	Results of soil with 10% moisture content simulation of 11 hours operation	40
5.4	Performance analysis of wet EATHE systems with 15% moisture content for summer cooling	40
5.4.1	Results of soil with 15% moisture content simulation of 1 hour operation	40

5.4.2	Results of soil with 15% moisture content simulation of 6 hours operation	41
5.4.3	Results of soil with 15% moisture content simulation of 11 hours operation	42
5.5	U-Shaped geometry results	43
5.5.1	Comparison of Straight shaped and U-shaped pipe geometry for dry soil 1 hour operation	44
5.5.2	Comparison of Straight shaped and U-shaped pipe geometry soil with 5% moisture content for 1 hour operation	45
5.5.3	Comparison of Straight shaped and U-shaped pipe geometry soil with 10% moisture content for 1 hour operation	45
5.5.4	Comparison of Straight shaped and U-shaped pipe geometry soil with 15% moisture content for 1 hour operation	46
5.5.5	Comparison of Straight shaped and U-shaped pipe geometry soil with 15% moisture content for 6 hours operation	47
5.5.6	Comparison of Straight shaped and U-shaped pipe geometry soil with 15% moisture content for 11 hours operation	47
5.6	Velocity variation of the EATHE system	48
6	CONCLUSION	49
6.1	Scope for Future work	50
	REFERENCES	51
Appendix A.1	Turbulence Models	54

Appendix A.2	Design of EATHE	64
Appendix A.2	Simulation data of dry and wetted EATHE	70

LIST OF FIGURES

Figure	Title	Page No.
1.1	Simple earth air tunnel heat exchanger	1
2.1	Scheme of the EAHX	9
2.2	Method used to remove condensed moisture	11
2.3	Scheme of the EAHX-HRV system	11
2.4	TRNSYS information flow diagram for the EAHE with SAHD.	13
2.5	Experimental set-up of EPAHE	14
3.1	Physical geometry details of EATHE system	16
3.2	Schematic of the EATHE system	20
3.3	Validation of outlet air temperature for 6 hours operation	21
4.1	Schematic of the experimental set up (wet tunnel)	22
4.2	Physical geometry details of EATHE system	23
4.3	Meshing of circular pipe	24
4.4	Temperature vs Length for different element size as a result of grid independence test	31
5.1	Variation of Temperature with length of dry soil for 1 hour operation	32
5.2	Variation of Temperature with length of dry soil for 6 hours operation	33
5.3	Variation of Temperature with length of dry soil for 11 hours operation	33
5.4	Variation of Temperature with length of soil with 5% moisture for 1 hours operation	34
5.5	Variation of Temperature with length of soil with 5% moisture for 6 hours operation	34
5.6	Variation of Temperature with length of soil with 5% moisture for 11 hours operation	35
5.7	Variation of Temperature with length of soil with 10% moisture for 1 hours	36

	operation	
5.8	Variation of Temperature with length of soil with 10% moisture for 6 hours operation	36
5.9	Variation of Temperature with length of soil with 10% moisture for 11 hours operation	37
5.10	Variation of Temperature with length of soil with 15% moisture for 1 hour operation	38
5.11	Variation of Temperature with length of soil with 15% moisture for 6 hours operation	39
5.12	Variation of Temperature with length of soil with 15% moisture for 11 hours operation	39
5.13	Variation of Temperature with length of soil with 15% and 18% moisture for 1 hours operation	40
5.14	Auto-cad geometry of U-Shaped EATHE	41
5.15	Ansys fluent geometry of U-Shaped EATHE	41
5.16	Variation of Straight shaped vs U-shaped geometry of dry soil for 1 hours operation	42
5.17	Variation of Straight shaped vs U-shaped geometry of soil with 5% moisture content for 1 hours operation	43
5.18	Variation of Straight shaped vs U-shaped geometry of soil with 10% moisture content for 1 hours operation	43
5.19	Variation of Straight shaped vs U-shaped geometry of soil with 15% moisture content for 1 hours operation	44
5.20	Variation of Straight shaped vs U-shaped geometry of soil with 15% moisture content for 6 hours operation	45
5.21	Variation of Straight shaped vs U-shaped geometry of soil with 15% moisture content for 11 hours operation	45
5.22	Velocity variation of dry soil one hour operation of EATHE system	46

LIST OF TABLES

Table	Title	Page No.
4.1	Physical and thermal properties of materials used in simulation	29
4.2	Physical and thermal properties of soil with different moisture content used in simulation	27

NOMENCLATURE

English Symbols

Notation	Description	Unit
$C_{p,a}$	Specific heat of air at constant pressure	$\text{J kg}^{-1} \text{K}^{-1}$
D, d	Pipe diameter	m
D_h	Hydraulic diameter of pipe	m
f	Friction factor	unit less
h_c	Convective heat transfer coefficient	$\text{Wm}^{-1}\text{K}^{-2}$
k_t	Thermal conductivity of tube	$\text{Wm}^{-1}\text{K}^{-1}$
k	Thermal conductivity of air	$\text{Wm}^{-1}\text{K}^{-1}$
L	Length of tube	l
\dot{m}	Mass flow rate of air	kg s^{-1}
Nu	Nusselt number	unit less
n	Number of parallel tube	unit less
Δp	Pressure loss	Bar
Pr	Prandtl number	unit less
r_i	Pipe radius	m
r_o	Radius of cylinder denoting thickness of soil surrounding pipe	M
Re	Reynolds number	unit less
Re_{DH}	Reynolds number calculated using the hydraulic diameter of the given area	unit less
T_{amb}	Temperature of ambient air	$^{\circ}\text{C}$
v	Velocity of air	m s^{-1}
V	Total volume flow rate	m^3

Greek Symbols

Notation	Description	Unit
ε	Effectiveness of EATHE	Unit less
ρ	Density of air	kg m^{-3}
ν	Kinematic viscosity of air	$\text{m}^2 \text{s}^{-1}$
μ	Dynamic viscosity of air	$\text{kg m}^{-1} \text{s}^{-1}$
μ_t	Dynamic turbulent viscosity or eddy viscosity	$\text{kg m}^{-1} \text{s}^{-1}$

LIST OF ABBREVIATIONS

AC	Air-conditioner
AFP	Air fan power
AGHX	Air-Ground Heat Exchanger
AHU	Air Handling Unit
ANN-HC	Artificial Neural Network based Heat Convection
ASHP	Air Source Heat Pump
ATEHE	Air-To-Earth Heat Exchanger
CAD	Computer Aided Design
CFD	Computational Fluid Dynamics
COP	Coefficient of Performance
DBT	Dry Bulb Temperature
DEC	Direct Evaporative Cooler
DHW	Domestic Hot Water
EAHE	Earth to Air Heat Exchanger
EAHX	Earth to Air Heat Exchangers
EATHE	Earth Air Tunnel Heat Exchanger
ETHE	Earth-Tube Heat Exchanger
FEM	Finite Element Method
FVM	Finite Volume Method
GA	Genetic Algorithm
GCC	Ground Coupled Circuit
GCHE	Ground Coupled Heat Exchanger
GCHP	Ground Coupled Heat Pump

GHE	Ground Heat Exchangers
GSHP	Ground-Source Heat Pump
HP	Horse Power
HGCHP	Hybrid Ground Coupled Heat Pump
HVAC	Heating, Ventilation and Air Conditioning
IRR	Internal Rate of Return
PDE	Partial Differential Equation
PUF	Polyurithane Foam
PV	Photo Voltaic
PVC	Poly Vinyl Chloride
RTD	Resistance Temperature Detector
RH	Relative Humidity of air
SAGCHP	Solar Assisted Ground Coupled Heat Pump
SPAHE	Soil Pipe Air Heat Exchanger
SHESS	Soil Heat Exchanger-Storage Systems
TIZ	Thermal Influence Zone
UGCHE	U-Vertical Ground Coupled Heat Exchanger
WBT	Wet Bulb Temperature

CHAPTER 1

INTRODUCTION

1.1 Background of EATHE system

The idea of using earth as a heat sink was known in ancient times. In about 3000 B.C., Iranian architects used wind towers and underground air tunnels for passive cooling. Earth–air heat exchangers have been used in agricultural facilities (animal buildings) and horticultural facilities (greenhouses) in the United States over the past several decades and have been used in conjunction with solar chimneys in hot arid areas for thousands of years, probably beginning in the Persian Empire. Underground air tunnel (UAT) systems, nowadays also known as earth to air heat exchangers (EAHEs), have been in use for years in developed countries due to their higher energy utilization efficiencies compared to the conventional heating and cooling systems. Implementation of these systems in Austria, Denmark, Germany, and India has become common since the mid-1990s and is slowly being adopted in North America.

Earth–air heat exchangers are one of the fastest growing applications of renewable energy in the world, with an annual increase in the number of installations with 10% in about 30 countries over the last 10 years. Except for Sweden and Switzerland, the market penetration is still modest throughout Europe but is likely to grow with further improvements in the technology and the increasing need for energy savings.

1.2 Passive Cooling Techniques

Passive cooling or heating systems, which make use of energy from nature such as sun, wind, earth, are well recognized for conservation of natural resources of energy and for their environmental friendliness. Passive systems use no or very little amount of commercial form of energy such as electricity, coal, oil or gas. Whereas, active systems are those that consumed a large amount of commercial energy. The natural means which can be used for passive cooling are:

- Natural Ventilation
- Shading
- Wind Towers

- Courtyard Effect
- Earth Air Tunnels
- Evaporative Cooling
- Passive Downdraft Cooling

The passive cooling systems have many advantages such as:

- System is of low cost
- Requires less maintenance
- System is simple
- Operation is natural
- System remains operative and effective as and when required

As far as life cycle cost is concerned, passive cooling systems are least expensive means of cooling/heating a home which maximizes the efficiency of the building envelope without any use of mechanical devices. All passive cooling technics rely on daily changes in temperature and relative humidity. These natural cooling techniques can reduce at least to some extent the peak cooling load of a building, thereby reducing the size of air conditioning plant.

1.3 Principle of EATHE system

Earth to Air Heat Exchanger system (EAHE) is one of the passive heating and cooling systems, having the relative advantage over rest of the most passive technics due to its ability to provide both the effects: heating in winter season and cooling during summer season. Earth behaves thermal storage medium. Due to higher thermal inertia of the earth, seasonal variations in temperature occur up to a depth of about 3-3.5 meters. Beyond this depth, the earth's temperature, therefore, remains constant. Usually, the value of this undisturbed soil temperature is equal to the annual average of ambient air temperature. Therefore, at a sufficient depth (i.e. below 3.5 m), the ground temperature is always higher than that of the outside air in winter and is lower in summer. earth air tunnel heat exchanger system (EATHE) as shown in Fig. 1.1.

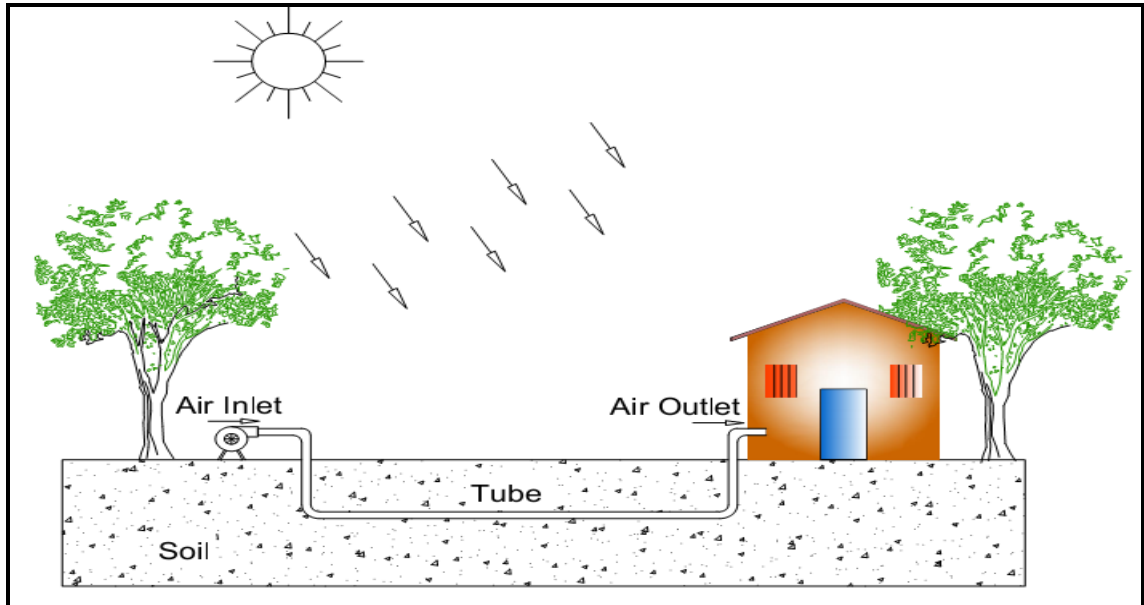


Fig. 1.1: Simple earth air tunnel heat exchanger

EATHE is a cooling/heating system which consists of metallic, P.V.C or concrete pipes buried in the ground through which outside or ventilation air is passed. Temperature difference between air and soil can be utilized to pre-cool or pre-heat ventilation air. Earth air tunnel heat exchanger may be an open loop system or closed loop system. In an open loop system, outdoor air is drawn through the EATHE pipes and conditioned air is supplied to space where it is required. Whereas, in a closed-loop system, air from the conditioned space is re-circulated through EATHE pipes and supplied back to space. Closed loop system does not exchange air with the outside. Usually the EATHE pipes are buried at a depth where the soil temperature does not vary much means remains about constant throughout the year. Hence, considering this aspect, air cannot be heated above the undisturbed soil temperature value, nor it can be cooled below undisturbed temperature. Earth behaves as a huge collector-cum-storage medium and can be used as daily or seasonal storage medium. The ground possesses many advantaged due to its high capacity as well as its insulation potential. With an average volumetric density of 1800 kg m^{-3} and thermal capacity of $920 \text{ Jkg}^{-1}\text{K}^{-1}$, each cubic meter of the ground, or rock bed, could store 1.67 MJ kg^{-1} . Heat loss from an underground reservoir is relatively small and the annual heat losses amount to about only 10% of the total annual collected energy. Similarly, the thermal capacity of the earth is such that the diurnal variations of the surface temperature do not penetrate much deeper than 0.5 m, and seasonal variations up to a

depth of about 3 meters. Beyond this depth, the earth's temperature, therefore, remains constant. The value of this temperature is usually seen to be equivalent to the all year mean of the soil air temperature of its surface. Measurements show that the ground temperature below a certain depth remains relatively constant throughout the year and the ground capacitance is regarded as a passive means of heating and cooling of buildings. This is due to the fact that the temperature fluctuations at the surface of the ground are diminished as the depth of the ground increases because of the high thermal inertia of the soil. Also, there is a time lag between the temperature fluctuations at the surface and in the ground. Therefore, at a sufficient depth, the ground temperature is always higher than that of the outside air in winter and is lower Earth to air tunnel heat exchangers are having a great potential for using as air conditioning system because of the following factors:

1. Lower cooling energy costs
2. Possibility to reduce or avoid a conventional cooling system
3. Low operating cost
4. Thus, by using an earth air-tunnel heat exchanger system, the energy and peak load requirements for space conditioning can be significantly reduced, offering large energy conservation opportunities

The use of earth as heat source and a heat sink with buried pipes or underground earth to air heat exchanger is a concept that has existed in Islamic and Persian architecture for many centuries. Such system has been repeatedly used in architectural design for natural conditioning of the air and maintaining internal thermal comfort. And earth to air heat exchanger consists of:

- a. Underground pipe
- b. Fan, to blow air
- c. Sieve, to filter the air, by preventing the entry of unwanted particles from the ground
- d. Tunnel fan

1.4 EATHE system with wet soil

It is understood that passive cooling/heating systems can not completely replace the active cooling/heating systems. Rather, the passive cooling/heating strategies, when effectively integrated with active systems, promote sustainability and energy saving. The ground heat exchangers are the relatively constant temperature geothermal sinks/source for heating or cooling purposes around the year.

In wetted EATHE system, An EATHE system is coupled with water trickling system. Since the thermal conductivity of soil largely depends on moisture content. Therefore, increasing the moisture of soil in the close vicinity of EATHE pipe will improve the soil thermal conductivity. In this system, the moisture present in the soil takes away much greater amount of heat from air flowing through the pipes, as specific heat of moisturising soil is much higher than that of dry soil. Therefore, greater drop in air temperature is achieved at much shorter pipe length.

1.5 Objectives of the present research

1. To determine the thermal performance of EATHE system with dry and wet soil using ANSYS FLUENT 15.0 and validate with secondary experimental results.
2. To study the effect of soil moisture variation on the thermal performance of EATHE system.

1.6 Scope of present research

1. In the present research, a CFD tool set up of Earth Air Tunnel Heat Exchanger system comprising of 61.5 m long, 0.1 m diameter PVC pipes, identical in all respect shall be developed.
2. Thermal performance of two EATHE systems, one with dry soil and another with wet soil shall be determined.

1.7 Thesis Organization

This thesis report is organized into five chapters.

1. In Chapter 1, the concept of EATHE and its application along with the terminology being used in the EATHE's performance analysis has been highlighted.
2. Chapter 2 consists of detailed literature survey and identifies the problem to be investigated.
3. Chapter 3 deals with the system description and simulation set up.
4. Chapter 4 contains the details of simulation procedure used in the study and different observations obtained and the results and performance analysis of EATHE system with dry and wet soil.
5. Chapter 5 includes conclusions from the study along with scope for further research.

CHAPTER 2

LITERATURE REVIEW

Introduction

Most of the EATHE systems have been developed as experimental units to explore their heating potentials, whereas, many of the researchers have simulated EATHE systems using simulation tools to visualize the effect of various parameters on the performance of these systems. Some of the mathematical models have also been presented by many researchers to analyses such systems. Some of the literature regarding the experimental as well as theoretical study of earth to air heat exchanger has been discussed below. The literature survey on these topics based on the studies carried out by various researchers is presented in this chapter.

- (i) Numerical or mathematical modelling
- (ii) Experimental investigations
- (iii) Modelling using computer simulation programs

2.1 Numerical or mathematical modelling

Modelling is a convenient way for performance analysis of any system without major investments in fabrication. Fluid flow and heat transfer problems can be modelled using fundamental laws and governing equations. Different mathematical methods such as finite difference method, finite element method, artificial neural network and genetic algorithm have been used for analysis of EATHE.

Trombe et.al. [1] have studied the performance on earth air heat exchanger system coupled with the residential buildings which are built in the south of France very near the city of Toulouse. The experimental results were validated with simplified model. From the experimental results, it was found that the system could be used to save the energy consumption of the house by 10% in preheating the fresh air during the winter period to avoid freeze risk in the dwelling and to maintain the comfort conditions in the summer days. Parametric studies were made to optimize the efficiency of the system.

A numerical model to calculate the performance of multiple and parallel earth air heat exchanger was described by **Mihalakakaou et al.** [2]. The system consisted of parallel, earth tubes, buried in the ground, through which indoor air was propelled and cooled by the bulk temperature of the natural ground. Four plastic pipes of 0.125 m radius and 30 lengths were buried in the ground at the depth of 1.2 m depth. They performed the experiment for 5,10 and 20 m/s air velocities while the other parameters unchanged. It is noticed that if they increased the mass flow rate then temperature increases at outlet of pipe of earth to air heat exchanger.

Kumar et al. [3] used the concept of goal-oriented genetic algorithm (GA) to design a tool for evaluating various aspects of EATHE behaviour. Impact of humidity, ambient temperature, ground surface temperature and ground temperature at certain depth on outlet temperature of EATHE was studied through sensitivity analysis. Outlet temperature was significantly affected by ambient air temperature, moisture content and ground temperature at burial depth.

Puri [4] evaluated the single pipe carrying hot fluid buried in the ground of medium wet sand by Parametric study for system variables pipe diameter, initial soil moisture concentration and temperature, and fluid-tube interface temperature using finite element model. It was found that temperature profiles developed faster in higher moisture soil than lower moisture soil. It was also pointed out that smaller diameter pipes are superior for enhancing the rate of heat transfer, though, the pressure drop was also higher in small diameter pipes.

Kumar et al. [5] presented a numerical model to predict energy conservation potential of earth air heat exchanger (EAT) system. This model improves upon previous studies by incorporating effects of ground temperature gradient, surface conditions, moisture content and various design aspects of EAT. The model is based on simultaneously coupled heat and mass transfer in the EAT and is developed within the scope of numerical techniques of Finite Difference and FFT (Matlab). The model was validated against experimental data of a similar tunnel in Mathura (India), and was then used to predict the tube-extracted temperature for various parameters such as humidity variations of circulating air, air flow rate and ambient air temperature. The model is found to be more accurate in predicting tube extracted temperature variations

along the length (error range $\pm 1.6\%$). They developed the, mathematical model as a transient axi-symmetric system.

Tzaferis et al. [6] carried out using eight different algorithms, Sensitivity analysis based on different parameters such as inlet air temperature, air velocity, pipe length, pipe radius and the pipe depth for evaluating the performance of earth-to-air heat exchangers. It was observed that changes up to a certain limit of length and diameter of the underground pipe and air velocity in the pipe impact the system performance.

Liu et al. [7] used volume-averaging method for developing a mathematical model for describing heat and moisture transfer in the porous soil with a dry surface layer. An experiment was conducted in a closed-loop wind tunnel to investigate the temperature effect on soil moisture transport. Theoretical and experimental results reveal that temperature and temperature gradient play an important role in moisture transport in soil.

Krarti and Kreider [8] did the parametric analysis of an underground air tunnel to determine the effect of tunnel hydraulic diameter (D_h) and air flow rate on the heat transfer between ground and air inside the tunnel. It was observed that an increase in the diameter resulted in a higher outlet air temperature. As the pipe diameter D_h increased, less heat was exchanged between a unit mass of air and the surrounding soil, resulting in a smaller decrease of the outlet air temperature.

Khandelwal et. al. [9] made a simple Excel based mathematical model for the design of EATHE systems for the ground floor of the library of the Malaviya National Institute of Technology Jaipur for meeting a given cooling/heating load. This model also helps in determining characteristic dimensions, number of pipes, air flow rate, selection of blower and economic investments in an EATHE system. A thermal comfort survey was also conducted to find the thermal comfort temperature in the library of MNIT, which is approx. 28.6°C , quiet near to the temperature obtained through this EATHE system.

2.2 Experimental investigations

A many of experimental work has been carried out for evaluating the performance of Earth Air Tunnel Heat Exchangers (EATHE) in all over world. To study the impact of different parameters affecting the performance of EATHE system and to validate the

results of simulations and mathematical modelling, various researchers had developed experimental set ups having different pipe diameters, different pipe materials, different lengths, laid at different depths in various ground conditions.

Khabbaz et al. [10] presented an experimental and numerical study of an EAHX for air cooling, connected to a residential building located in Marrakech (Morocco) which climate is a hot semi-arid one. The EAHX consists of three parallel PVC pipes of 72 m length each and 15 cm inside diameter, buried at 2.2-3.2 m depth as shown in Fig. 2.1. Each pipe is equipped with a fan, which blows treated air into the building. The experimental study consists of summer monitoring of the EAHX via measurements of air temperature and humidity throughout the exchanger, as well as at its inlet and outlet to the building for two fixed values of the airflow rate.

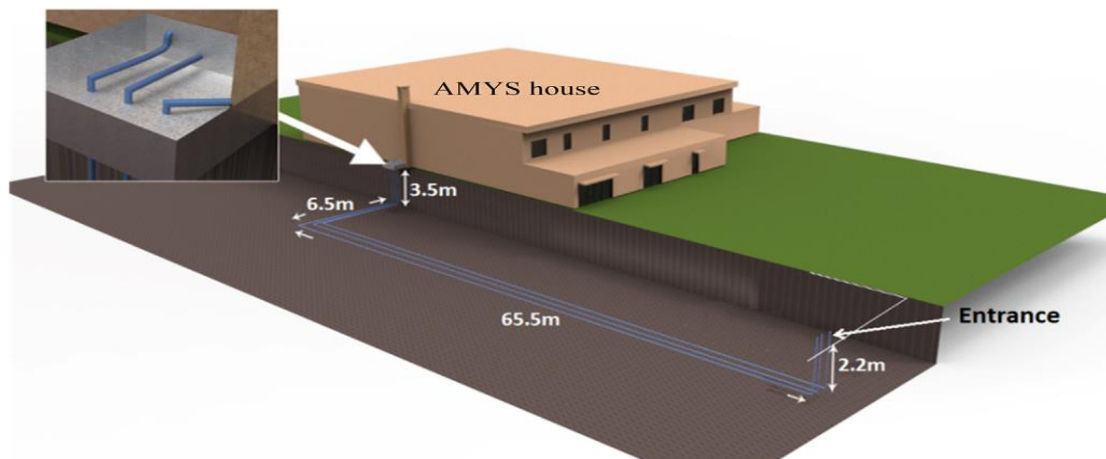


Fig. 2.1 Scheme of the EAHX

The experimental results show that the EAHX is a good semi passive system for air refreshment, as the recorded blown air temperature into the building is quasi constant at 25 °C with air humidity around 40%, even though the outside temperature reaches more than 40 °C. Furthermore, the reduction of daily and annual air temperature amplitudes is characterized by an exponential drop as a function of pipe length. The characteristic length is found to be around 20 m and 70 m respectively for the daily and annual air temperature amplitudes reduction. Moreover, it is shown that the design guidelines from literature cannot straightforwardly be applied to an EAHX which is subject to meteorological disturbance from the upper surface and/or which is not operated all year round, for which numerical simulation with a validated model remains necessary.

Sharan and Jadhav [11] analysed Performance of a single pass Earth-Tube Heat Exchanger (ETHE) in cooling and heating mode, for an ETHE of 50 m long mild steel pipe, 10 cm nominal diameter and 3 mm wall thickness, at depth of 3 m. Ambient air was passed through the pipe by a 400 W blower. Air velocity in the pipe was 11 ms^{-1} . It was found that the ETHE could reduce the temperature of hot ambient air by as much as 14°C in May when soil temperature was 26.6°C .

Ozgener [12] experimentally determined the exergetic performance of an underground air tunnel used for greenhouse cooling. The daily maximum cooling coefficient of performances (COP) values was obtained to be 15.8. The total average COP in the experimental period was 10.09. The system COP was calculated based on the amount of cooling produced by the air tunnel and the amount of power required to move the air through the tunnel, while the exergetic efficiency of the air tunnel was found to be in a range among 57.8 - 63.2%.

Misra et al. [13] investigated experimentally hybrid mode of EATHE. They performed two modes of operation. In first mode outlet air of EATHE is directly sent to the room with AC unit coupled. In second mode of operation the outlet air is used to cool the condenser tube. It was found that second mode of operation showed better performance than first mode, saving 12 % more energy consumption.

Vlad et. al. [14] did their experiments on two different types of earth to air heat exchangers in Bucharest where outside air temperature ranges from -15°C to 40°C while soil temperature has a lower range only 4°C to 18°C . They used two different types of heat exchangers. The first one with the air flowing inside the tube and a second one with brine. They designed a house without a basement like "Politechnica house". A condensation tower was built at the lowest point of the earth to air heat exchanger, close to the wall. The condensed moisture is removed by a condensed pump as shown in Fig. 2.2. They told that the house is ventilated with fresh air; the heating load during winter becomes higher. To reduce energy consumption for heating, the air is preheated in two steps, first in the ground heat exchanger and second in a heat recovery unit (HRV) which can save even more than 90 % from the energy of exhausted air as presented in Fig. 2.3. The HRV system consists in a plate heat exchanger and two fans, the fans are identical, synchronized so that the basic

ventilation conditions to be fulfilled. Inside the PHE the exhausted air transfers heat to the supply air.

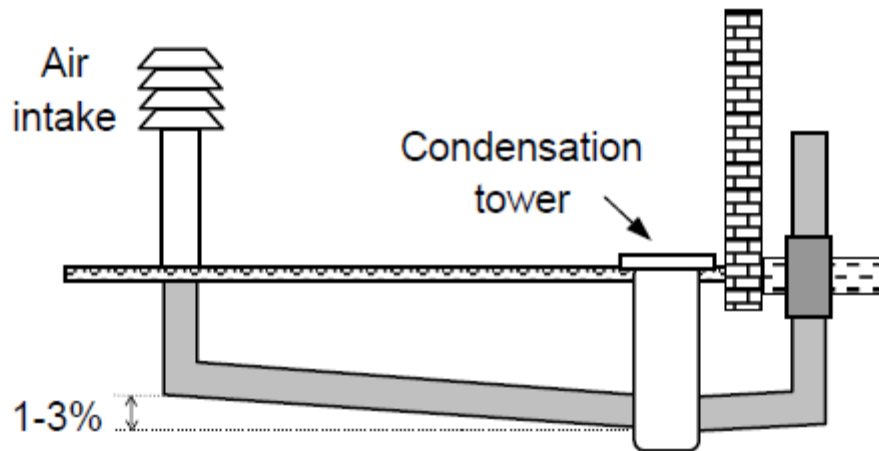


Fig. 2.2 Method used to remove condensed moisture

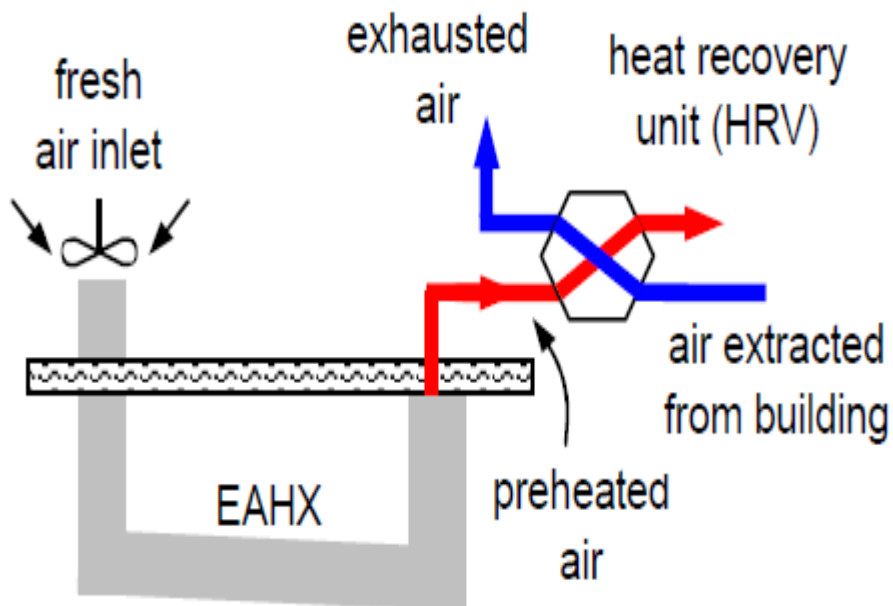


Fig. 2.3 Scheme of the EAHX-HRV system

They also prepared a theoretical model of EAHX. This model presents the algorithm for calculation of optimum value for length of the pipe integrated in an EAHX. From this they found out value of tube outlet air temperature which was very important

input parameter & it takes into consideration both the air temperature & soil temperature. The value of the tube outlet air temperature ($T_{a,o}$) is found by using the expression of the tube thermal efficiency:-

$$\epsilon = \frac{t_{a0} - t_{ai}}{t_s - t_{ai}}$$

From all these parameter, they found the thermal efficiency of the pipe varies between 0.5 & 0.99. They also take economic aspects into consideration. They decrease electrical energy consumption & increase thermal efficiency of EAHX.

Singh et al. [15] evaluated energy conservation in a cinema hall at Jodhpur (India) due to evaporative cooling, wind tower and earth air tunnel by conducting experiments. The effects of occupants, infiltration and lighting load had been taken into account. It was observed that the load on the air-conditioner was significantly reduced by using earth air tunnel heat exchanger. They also evaluated reduction in load using evaporative cooling.

2.3 Modelling using computer simulation programs

In recent years, focus on analysis of Earth Air Tunnel Heat Exchangers has shifted towards computer based studies. Tremendous work has been done on energy simulation program APACHE, TRNSYS, ENERGY PLUS for EATHE system. Benkert et al. [21] developed a computer based design tool GAEA which can be utilised as of design and optimization of earth air heat exchangers for building. Researchers are emphasizing on the use of computers for solving the equations of fluid flow through pipes and heat transfer taking place in it. Among these methods, Computational Fluid Dynamics (CFD) simulation is a better technique for carrying out the analysis of fluid flow and heat transfer problems because fluid flow and heat transfer can be observed using animations.

Bansal et. al. [16] has studied the underground temperature characteristics of the soil surrounding the EATHE pipe and the effect of duration of operation of EATHE on its thermal performance. Three different types of soils S1, S2 and S3 whose conductivities are 0.52, 2 and 4 W m⁻¹ K⁻¹ respectively have been considered. The heat transfer to outer soil by soil S1, S2 and S3 are 1%, 48.5% and 83.5% of total heat transfer through EATHE pipe respectively has been recorded in this study. Maximum

deterioration in the thermal performance in terms of temperature drop obtained by the studied EATHE system during continuous operation of 24 h is 0.7, 1.6 and 2.9 K for soil with thermal conductivity of 4, 2 and 0.52 W m⁻¹ K⁻¹ respectively.

Benhammou et. al. [17] evaluated the performance of EATHE coupled to a wind tower. This passive system simulated and operated under the climatic conditions of the Algerian desert in July, when the ambient temperature passes the 45°C. This survey allowed to approve the feasibility of such system for passive cooling of buildings and examining the influence of the geometric parameters of the EATHE as well as the wind tower on the thermal performance of the system.

Jakhar et al. (2016) [18] presented a model to estimate the heating potential for EAHE system with and without SAHD. The model was generated using TRNSYS 17 simulation tool and validated against experimental investigation on an experimental set-up in Ajmer, India. The experiment was done during the winter season, where the system was evaluated for different inlet flow velocities, length and depth of buried pipe. From the experimentation, it was observed that the depth of 3.7 m is sufficient for pipe burial and the 34-m length of pipe is sufficient to get optimum EAHE outlet temperature. It was also observed that increase in flow velocity results in drop in EAHE outlet temperature, while room temperature was found to increase for higher velocities (5 m/s). The COP of the system also increased up to 6.304 when assisted with solar air heating duct. The results obtained from the experiment data are in good agreement with simulated results within the variation of up to 7.9%. A simplified information flow diagram for the EAHE with SAHD system under investigation is shown in Fig. 2.4.

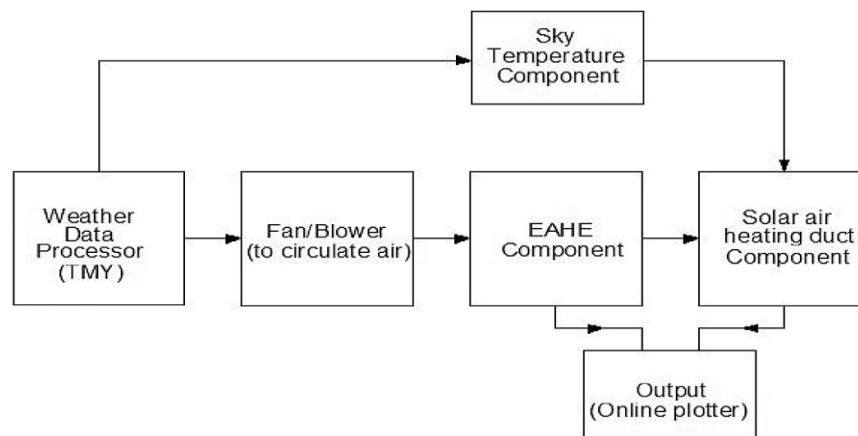


Fig. 2.4. TRNSYS information flow diagram for the EAHE with SAHD

Bansal et.al [19] designed a transient and implicit model based computation fluid dynamics (CFD) was developed to predict the thermal performance & heating capacity of earth -air-pipe heat exchanger system. The model is developed inside the FLUENT Simulation. The EPAHE is as shown in Fig. 2.5 comprises of two horizontal cylindrical pipes of 0.15 m inner diameter with buried length of 23.42 m made of up of PVC and mild steel pipes and buried at a depth of 2.7 m in a flat land with dry soil. The two pipes viz. PVC and steel are connected to common intake and outlet manifold for air passage. Six thermocouples are inserted at fixed distance along the length of each pipe at T₁, T₂, T₃, T₄, T₅ and T₆, to measure temperature of the air along the length of each pipe.

The model is validated against experimental investigations and experimental, set-up in Ajmer (western India). Good result obtained between simulated & experimental data.

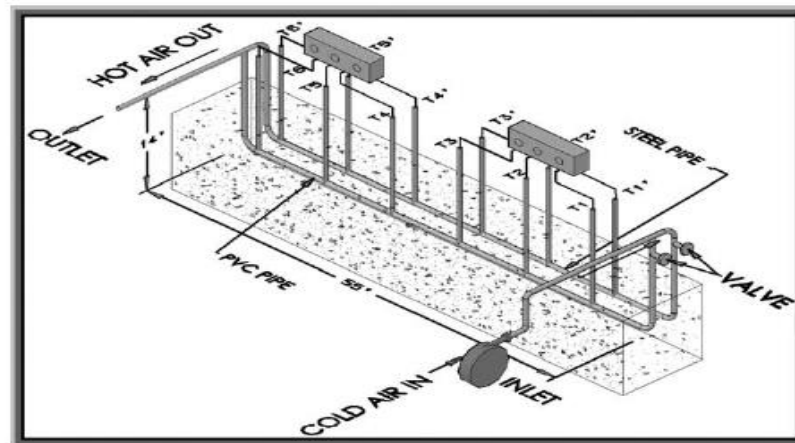


Fig. 2.5 Experimental set-up of EPAHE

In this EPAHE gives the heating in the range of 4.1-4.8 °C for the flow velocities 2-5 m/sec. Validated of simulated temperature with experimental results. They find the variation in simulated and experimental results ranges from 0 to 2.07 % for different sections along the length of pipe for steel pipes and for PVC pipes are 0 to 1.2 %.

2.4 Summary of Literature Review

After undergoing detail literature survey following things were observed and used in the present study.

- a) Instead of using large diameter pipe in EATHE system, pipes of smaller diameter (4" to 6") should be used for comfort requirements. Smaller diameter pipes not only enhance performance of EATHE, but are also cheaper as compared to large diameter pipes. It also gives a larger temperature drop.
- c) Maximum heat transfer takes place between subsoil and air in case of smallest pipe; therefore, for the same length of pipe, the greater cooling effect is obtained in case of smaller diameter pipes.
- d) Temperature of air reduces sharply along the section of pipe initially and after a certain length of pipe this decrement is very small.
- e) Temperature of air reduces sharply along the section of pipe in case of smaller dia. Pipe.
- f) Sandy wets clay loam (heavy clay) has a higher cooling more potential than dry sandy soil. Sandy soil has higher heating potential in desert areas.
- g) Pipe material has little effect on thermal performance.
- h) The temperature 29.5-31.5 °C can be achieved through using EATHE system alone or integrated with other system.
- i) If thermal adaptation of occupants with prevailing ambient temperature is considered, then EATHE system or integrated with desert cooler can maintain comfort band throughout the year.

CHAPTER 3

System description and simulation setup

The thermal performance of an EATHE system (under transient conditions) has been evaluated using research Computational Fluid Dynamics software package, ANSYS FLUENT v 14.5. It has the capabilities to predict the incompressible, compressible, laminar and turbulent fluid flow along with buoyancy and compressibility phenomena. FLUENT turbulence models can predict the turbulence behaviour near wall via the use of extended wall functions.

3.1 Physical Model

The physical geometry of EATHE systems, including pipe and surrounding soil were modelled (Figure 3.1) using ANSYS's workbench platform i.e. ANSYS's DESIGN MODELER. Developed physical model of EATHE system was meshed using 3D hybrid (hexahedral and tetrahedral) meshing comprised of total 654838 cells (elements) in ANSYS's workbench MESHING.

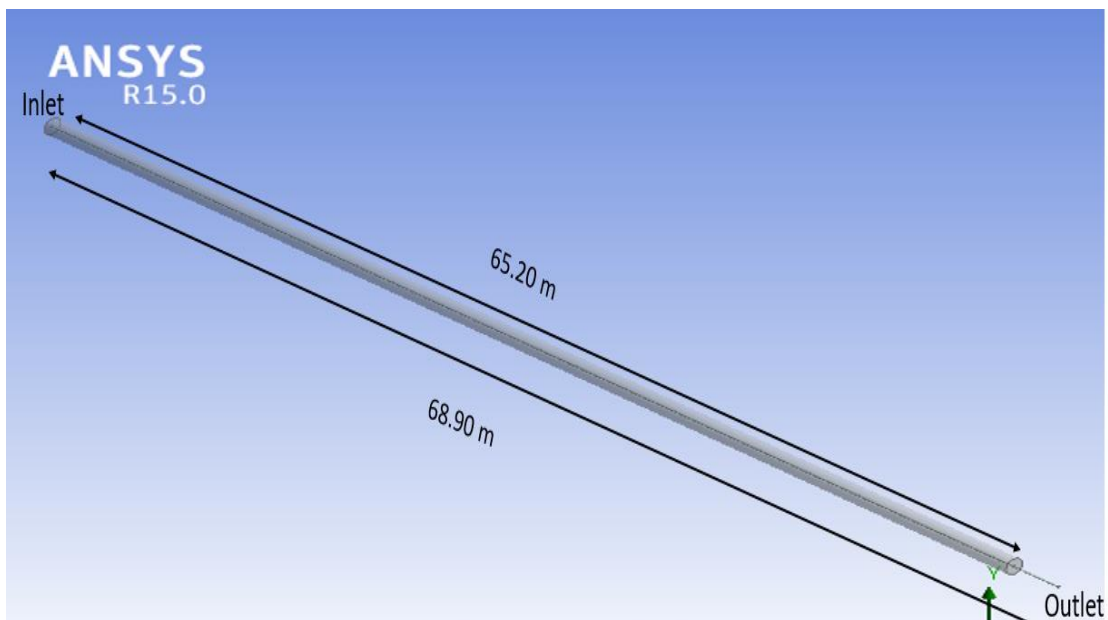


Figure 1 Physical geometry details of EATHE system

3.2 Simulation model

ANSYS FLUENT v 14.5 was used in the study that used the finite volume method to convert the governing equations into numerically solvable algebraic equations. The numerical investigations were based on the following assumptions:

- i. Thermo-physical properties of soil, pipe and air remain constant during operation.
- ii. Thermal contact between soil and buried pipe is perfect.
- iii. Initially, soil and pipe temperature is considered equal and undisturbed.
- iv. Air inside an EATHE mixes evenly within each segment along the tube without stratification.

3.2.1 Governing Equations

The present numerical model consists of the continuity equation, the momentum equation, the energy equation and the realizable k- ϵ equation and these can be expressed in the following conservative form.

$$\frac{\partial \rho}{\partial t} + \nabla \cdot (\rho \vec{v}) = S_m \quad (1)$$

Where; ρ is the density of the fluid (kg m^{-3}) and \vec{v} is the velocity vector of the flow (m s^{-1}). The source term S_m is the mass added or removed by the continuous phase dispersed phase or any other source ($\text{kg m}^{-3}\text{s}^{-1}$).

$$\frac{\partial}{\partial t} (\rho \vec{v}) + \nabla \cdot (\rho \vec{v} \vec{v}) = -\nabla p + \nabla \cdot (\bar{\tau}) + \rho \vec{g} + \vec{F} \quad (2)$$

where p is fluid static pressure (N m^{-2}), $\rho \vec{g}$ is the gravitational body force per unit volume (N m^{-3}), \vec{F} represents external body forces per unit volume (N m^{-3}), and $\bar{\tau}$ is the viscous stress tensor related to surface forces on an infinitesimal element of fluid (N m^{-2}), which is defined by:

$$\bar{\tau} = \mu \left[(\nabla \vec{v} + \nabla \vec{v}^T) - \frac{2}{3} \nabla \vec{v} I \right]$$

Where μ is the molecular viscosity ($\text{kg m}^{-1}\text{s}^{-1}$) and I is an unitary tensor.

In energy equation (Eq. 3), the terms on the left correspond to the local variation of energy and the advective transport of energy, respectively. The first three terms on the right side represent the energy transfer due to heat diffusion, mass diffusion and viscous dissipation, respectively. The last term, S_h (W m^{-3}), takes into consideration any source or sink of heat by conversion of any mode of energy (electrical, chemical) in thermal energy [19].

$$\frac{\partial}{\partial t}(\rho E) + \nabla \cdot (\vec{v}(\rho E + p)) = \nabla \cdot (\kappa_{eff} \nabla T - \sum h_j \vec{J}_j + (\bar{\tau}_{eff} \cdot \vec{v})) + S_h \quad (3)$$

$$E = h - \frac{p}{\rho} + \frac{v^2}{2}, \quad h = \sum_j Y_j h_j + \frac{p}{\rho}, \quad h_j = \int_{T_{ref}}^T C_{pj} dT$$

where E is the specific energy (J kg^{-1}), h is the sensible enthalpy (J kg^{-1}), Y_j and h_j are the mass fraction and the enthalpy of species j , respectively, c_{pj} is the specific heat of species j ($\text{J kg}^{-1}\text{K}^{-1}$), T_{ref} is a reference temperature ($T_{ref} = 298.15 \text{ K}$), κ_{eff} is the effective conductivity ($\text{W m}^{-1}\text{K}^{-1}$) given by $k + k_t$ being k_t the turbulent thermal conductivity defined according to the turbulence model adopted and \vec{J}_j is the diffusive flux of species j ($\text{kg m}^{-3}\text{s}^{-1}$).

To predict the turbulence inside the pipe, pressure based realizable k - ϵ model with enhanced wall treatment and energy equation is also solved with ANSYS since the computations included heat transfer. The k - ϵ model is one of the most common turbulence models, which is built in FLUENT and gives good results for bounded wall and internal flows with small mean pressure gradients.

$$\frac{\partial}{\partial t}(\rho k) + \frac{\partial}{\partial x_j}(\rho k u_j) = \frac{\partial}{\partial x_j} \left[\left(\mu + \frac{\mu_t}{\sigma_k} \right) \frac{\partial k}{\partial x_j} \right] + G_k + G_b - \rho \epsilon - Y_M + S_k$$

$$\frac{\partial}{\partial t}(\rho \epsilon) + \frac{\partial}{\partial x_j}(\rho \epsilon u_j) = \frac{\partial}{\partial x_j} \left[\left(\mu + \frac{\mu_t}{\sigma_\epsilon} \right) \frac{\partial \epsilon}{\partial x_j} \right] + \rho C_1 S_\epsilon - \rho C_2 \frac{\epsilon^2}{k + \sqrt{\nu \epsilon}} + C_{1\epsilon} \frac{\epsilon}{k} C_{3\epsilon} G_b + S_\epsilon$$

Where

$$C_1 = \max \left[0.43, \frac{\eta}{\eta + 5} \right], \eta = S \frac{k}{\epsilon}, S = \sqrt{2S_{ij}S_{ij}}$$

In these equations, G_k represents the generation of turbulence kinetic energy due to the mean velocity gradients, G_b is the generation of turbulence kinetic energy due to buoyancy. Y_M , represents the contribution of the fluctuating dilatation in compressible turbulence to the overall dissipation rate. C_1 and $C_{1\epsilon}$ are constants. S_k and S_ϵ are user-defined source terms.

The molecular Prandtl number Pr , turbulent kinetic energy k and turbulent dissipation rate ϵ are calculated by FLUENT automatically according to the physical parameter and flow velocity.

3.2.2 Boundary and initial condition

PVC pipe wall and surrounding soil were ‘Coupled’ in order to enable heat transfer and their initial temperatures were set according to the experimentally measured values. The air inlet boundary condition was specified as ‘Velocity Inlet’ and kept constant at 5 m/s. Air is a compressible fluid so ‘Pressure Outlet’ condition was specified for the air outlet.

3.2.3 Convergence and grid independence test

The convergence criteria were achieved for continuity, x-velocity, y-velocity, z-velocity, $k - \epsilon$ ($1e-3$) and the energy equation ($1e-6$) at the each time step. The grid independent size was determined by increasing the number of meshes until the criterion $\frac{\dot{p} - \dot{p} + 1}{\dot{p}} < 10^{-3}$ was satisfied. Here \dot{P} represents the calculated temperature using current mesh size and $\dot{P} + 1$ correspond to temperature using the next mesh size. For the grid independent, the air temperature was evaluated at the outlet of the EATHE system.

3.3 Model validations

3.3.1 Introduction of existing experimental facility

Experimental set-ups of simple (dry) and wetted earth air tunnel heat exchanger have been developed at the backyard of main building of Govt. Engineering College, Ajmer, India. Two identical Earth air tunnel heat exchanger systems were set up at the backyard of main building of Govt. Engineering College, Ajmer (India), parallel to each other of size 30 m x 1.5 m x 3.7 m, having similar dimensions to each other in all respects like length was 30 m, depth was 3.7 m and width was 1.5 m. Initially trenches were excavated having a depth of 3.7 m and a temperature sensor (4 wire RTD) was placed into it and pit was back filled with the sand. Temperature indicated by the sensor was measured and recorded on hourly basis for a fortnight, to observe the variation in the sub soil temperature. It was noticed that the temperature of sub soil remained constant at 300.2 K irrespective of time of the day. This temperature was nothing but the undisturbed ground temperature.

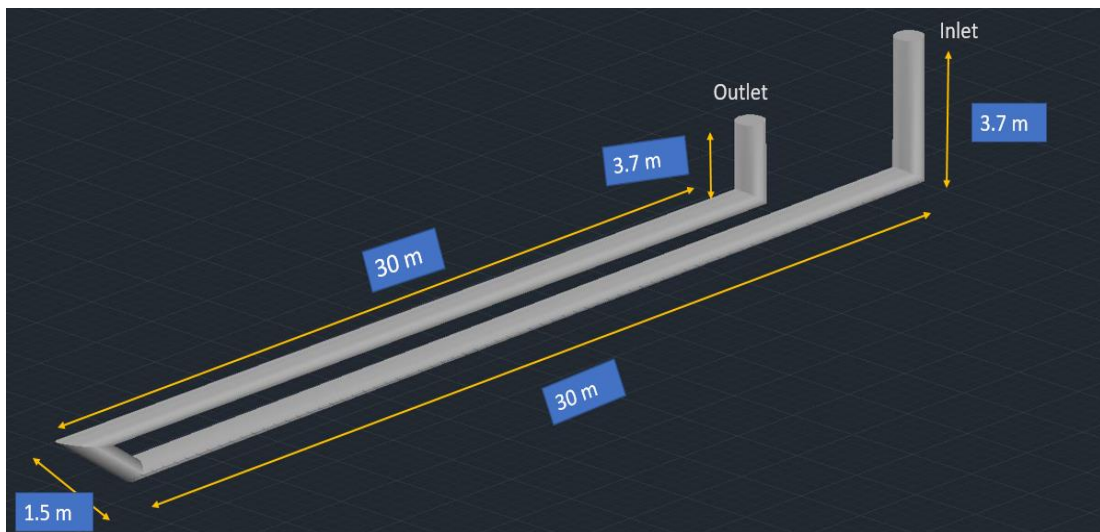


Figure 3.2 Schematic of the EATHE system

3.3.2 Comparison between numerical model and experimental model for validation

The initial soil and air temperature were known for the entire duration of EATHE operation. The EATHE inlet air flow velocity was kept constant at 5 m/s during the whole operation time. Figure 3.3 shows the variation in measured and simulated outlet air temperature for different moisture contents. A good agreement exists between measured and simulated outlet air and soil

temperatures. The maximum temperature difference observed was 3.1°K. This agreement establishes the validity of proposed model used for the simulation and was considered appropriate for further analysis.

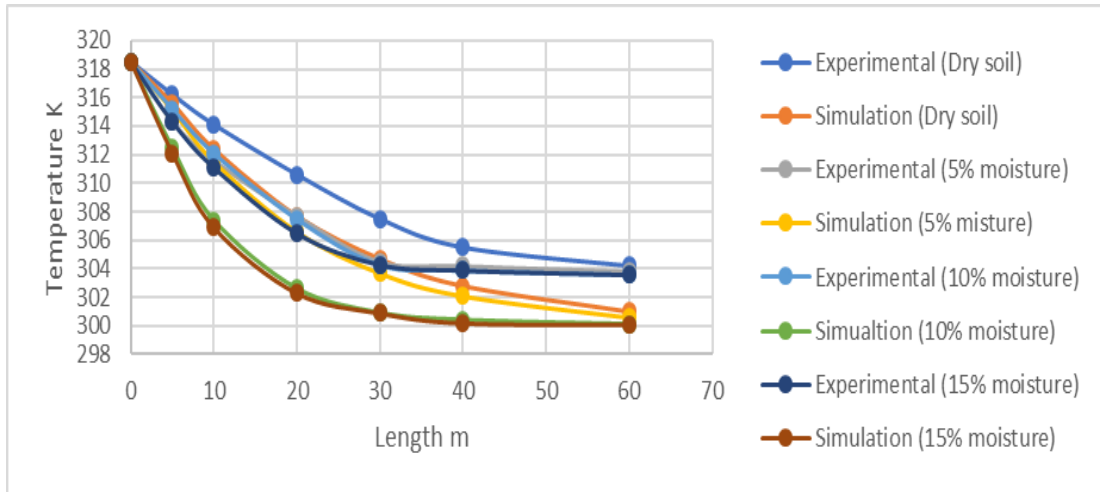


Figure 3.3 Validation of outlet air temperature for 6 hours operation

Chapter 4

CFD Modeling and Simulation

The CFD model was prepared in ANSYS Fluent 15.0.7 using dimensions of the EATHE system experimentally investigated by researchers, Kumar et. at [4]. He developed the experimental set-ups of simple (dry) and wetted earth air tunnel heat exchanger at the backyard of main building of Govt. Engineering College, Ajmer, India for the performance study.

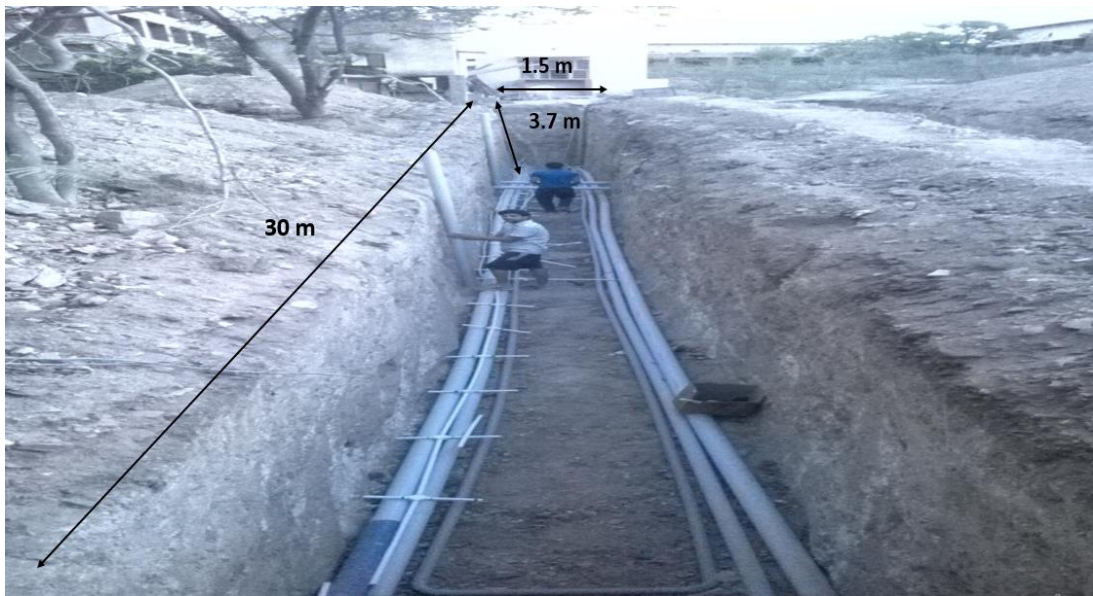


Figure 4.1 Schematic of the experimental set up (wet tunnel)

Two identical Earth air tunnel heat exchanger systems was developed at the backyard of main building of Govt. Engineering College, Ajmer (India), parallel to each other of size 30 m x 1.5 m x 3.7 m, having similar dimensions to each-other in all respect like length was 30 m, depth was 3.7 m and width was 1.5 m. Initially trenches were excavated having a depth of 3.7 m and a temperature sensor (4 wire RTD) was placed into it and pit was back filled with the sand. Temperature indicated by the sensor was measured and recorded on hourly basis for a fortnight, to observe the variation in the sub soil temperature. It was noticed that the temperature of sub soil remained constant at 300.2 K irrespective of time of the day. This temperature was nothing but the undisturbed ground temperature. Based on observed value of undisturbed sub soil temperature, it was decided to excavate the trench having depth of 3.7 m for laying the EATHE pipe.

4.1 Geometric Modeling

The geometric model of simple EATHE system was made using ANSYS version 15.0.7. The meshing of the generated model is carried out using ANSYS ICEM CFD. The geometrical model has been created for simple(dry) tunnel having pipe length 68.9 m length and diameter 0.01m while the soil volume created as concentric cylinder over the pipe having length 65.2 m and diameter 0.1m. One end of the pipe is the inlet of air while the other end of the pipe is the outlet.

In the experimental part, outlet is insulated hence no heat transfer is consider in the outlet. To keep the same working condition in simulation study, we removed the soil from pipe in the outlet part as shown in figure 4.2.

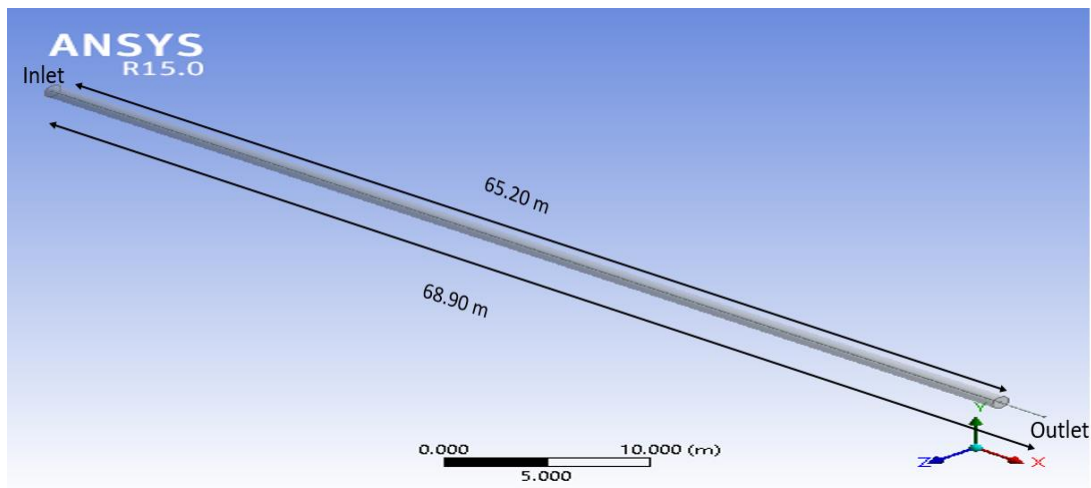


Figure 4.2 Physical geometry details of EATHE system

4.2 Meshing

The partial differential equations that govern fluid flow and heat transfer are not usually amenable to analytical solutions, except for very simple cases. Therefore, in order to analyse fluid flows, flow domains are split into smaller sub-domains (made up of geometric primitives like hexahedron and tetrahedron in 3D and quadrilaterals and triangles in 2D). The governing equations are then discretized and solved inside each of these sub-domains. Typically, one of three methods is used to solve the approximate version of the system of equations: finite volumes, finite elements, or finite differences. Care must be taken to ensure proper continuity of solution across the common interfaces between two sub-domains so that the approximate solutions inside various portions can be put together to give a complete picture of fluid flow in

the entire domain. The sub-domains are often called elements or cells, and the collection of all elements or cells is called a mesh or grid. In this CFD analysis, FLUENT version 15.0.7 [ANSYS] has been used and the FLUENT computation adopts a finite-volume approach to solve the conservation form of the governing flow equations. The geometry is shown in fig. 4.3 has been generated for the analysis of circular pipe of EATHE system. Similar procedures have been used to generate model and meshing for different cases.

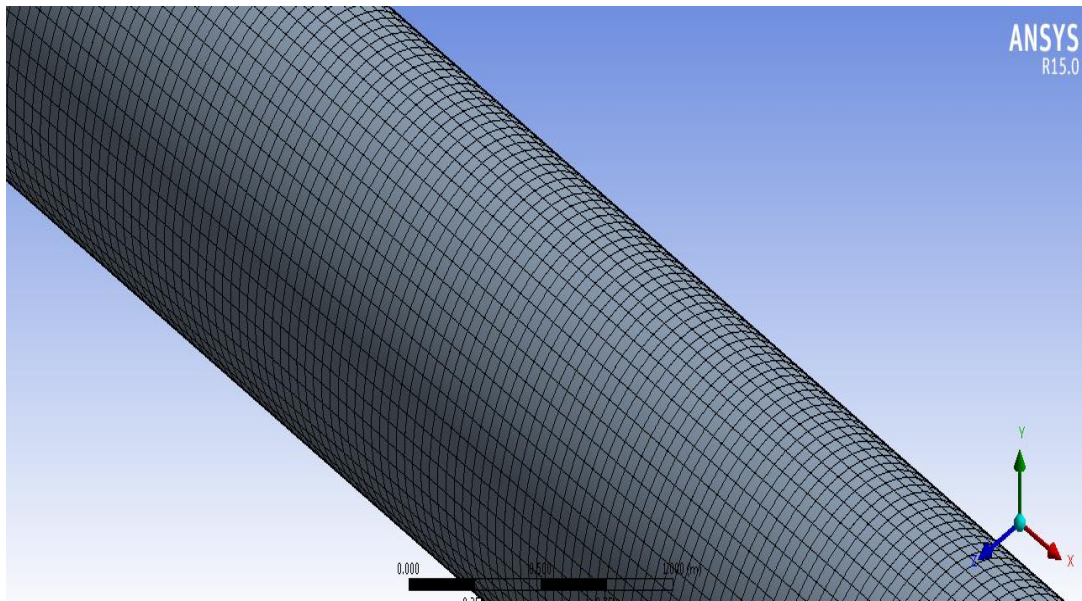


Figure 4.3 Meshing of circular pipe

4.3 Numerical solution and setup

Assumptions considered in CFD simulation are as follows:

- i. Thermo-physical properties of soil, pvc pipe and air remain constant during operation.
- ii. The vertical pipes are well insulated and no heat transfer is considered in the outlet section.
- iii. Thermal contact between soil and buried pipe is perfect
- iv. Air flow through the test section is fully developed.
- v. No slip condition for velocity is applied to the pipe surface.
- vi. Air inside EATHE mix evenly within each segment along the tube

- vii. The soil surrounding the pipe is isotropic, with homogenous thermal conductivity in all ground strata.
- viii. The thermal resistance of the pipe material is negligible (thickness of the pipe is very small).
- ix. The pipe is of uniform circular cross-section.
- x. The thermal effect of soil surrounding the pipe is negligible after a distance '10r' from the pipe outer surface, where 'r' is the pipe radius

4.3.1 Numerical solver used

FLUENT has two major numerical solvers; namely, segregated solver and coupled solver (implicit and explicit type). In either of these methods, FLUENT solves the governing integral equations for the conservation of mass, momentum and energy (when appropriate). Apart from these equations, other equations involving scalar quantities such as, turbulence and chemical species can also be solved in FLUENT and in all the cases a control volume based technique is used. In the present study of CFD analysis segregated solver was used. In the segregated algorithm, the individual governing equations for the solution variables (velocity, temperature, pressure, turbulent kinetic energy, etc.) are solved one after another. Each governing equation, while being solved, is "decoupled" or "segregated" from other equations. The segregated algorithm is memory-efficient, since the discretized equations need only be stored in the memory one at a time. Due to memory efficiency of the solver, it has been considered in the present case.

In this approach, the governing equations are solved sequentially (i.e., segregated from one another), because the governing equations are non-linear and coupled, therefore, several iterations of the solution loop are required to be performed before getting a converged solution. In this CFD analysis, air flows through the rectangular duct. There is heat transfer between the heating plate and the air flowing through the duct. By defining appropriate operating conditions, boundary conditions, solution parameters and convergence criteria, a converged numerical solution is obtained for each step. Different solution variables such as velocity, temperature, pressure, the turbulent kinetic energy of the flow was analysed in each step using the sequential results of the CFD simulation.

4.3.2 Solution Technique

Solution of the equations governing scalars (e.g. temperature, pressure, species concentrations) requires a discretization scheme (Versteeg, 1995). The two schemes relevant for this work are:

- First Order Upwind, in which cell face values are set equal to the cell centre value in the cell up-stream, and
- Second Order Upwind, in which the cell face values are calculated using a Taylor Series expansion to give an increased range of influence of the surrounding cells.

The Fluent User Guide (Fluent Incorporated) advises that the First Order scheme gives a stable solution with a good rate of residual convergence, with the limitation that the accuracy of the solution may not be satisfactory while the second order upwind scheme will result into more accurate solution. Therefore, second order upwind scheme has been adopted to get more accurate results.

4.3.3 Turbulence Model

Turbulence models are needed to solve unknown variables. No single turbulence model can be universally applied to all situations. Some consideration must be taken when choosing a turbulence model including; physics encompassed in the flow; level of accuracy; and computation resources available. Several turbulence transport models will be examined and discussed in this section. Both the Realizable and RNG (Renormalization Group) k - ϵ models along with the standard k - ϵ turbulence models were tested.

The largest challenge of CFD modelling lies on correct analysis of turbulent flow. Turbulence can be characterized as a chaotic state of fluid motion. It is characterized in terms of irregularity, diffusivity, large Reynolds numbers, three-dimensional vorticity fluctuations, dissipation and continuum. Because all airflows through a duct in which Reynolds number is larger than 4000 can be defined as turbulent ones, the CFD program used for airflow analysis and prediction requires appropriate models for turbulence. Generally, turbulent flows are analysed by three approaches:

- a) Direct Numerical Simulation (DNS),
- b) Large Eddy Simulation (LES), and

c) Turbulence Transport Models.

The DNS method requires very fine space discretization with cell size of the order of 10^{-3} m. Looking to the computation power of today's computers, simulations of such a finely meshed airflows are not realistic with this method. The LES method was developed by Deardorff (1970) who hypothesized that the turbulent motion could be separated into large and small eddies and that the separation between these two does not have a significant effect on the evolution of large eddies. Because this method assumes that small eddies are independent of the flow geometry, the need for a very fine grid is eliminated. The main contribution to turbulent transport comes from the large-eddy motion and, therefore, this method provides better results than methods which are based on empirical turbulent transport models. However, this method requires large computer power and memory. Therefore, LES is still rarely applied for the simulation of airflows. Therefore, like DNS, LES requires computers that are more powerful than those typically available today to be effectively applicable to airflow simulation.

Because of the difficulties involved in deterministic turbulence models i.e. DNS, LES, turbulence transport models are widely used in engineering applications. All the turbulence transport models solve the Reynolds statistically averaged Navier-Stokes (RANS) equations. These models can be generally divided into two categories:

- Reynolds stress models, and
- Eddy-viscosity models.

Reynolds stress models use transport equations for the individual Reynolds stress, while the eddy-viscosity models use Boussinesq approximation that relates Reynolds stress to the mean rates of deformation through an "eddy" viscosity. Reynolds stress models are applied to predict room airflow patterns in a room with jets. The results indicate that the Reynolds stress model is superior to the standard $k-\epsilon$ model, which is eddy viscosity model, because anisotropic effects of turbulence are considered. However, Chen (1996) compared three Reynolds-stress models with the standard $k-\epsilon$ model for natural convection, forced convection, mixed convection, and impinging jet in a room. He concluded that the Reynolds stress models are only slightly better than the $k-\epsilon$ model. Nevertheless, the Reynolds stress models require three to ten times

more computing time than the eddy-viscosity models because of the greater algebraic complexity. Thus, with the increase of computing time and relatively small improvement in indoor airflow prediction, Reynolds stress models are still very rarely applied in building simulations.

Classic eddy-viscosity models include mixing-length models such as the zero equation, one equation, and two equations eddy-viscosity model (Rodi1993). The two-equation model, often referred to as the “standard” $k-\varepsilon$ model, is the most widely-used turbulence model in engineering practice. Here, k represents the turbulence kinetic energy, while ε represents the dissipation rate of turbulence energy. There are several variations of $k-\varepsilon$ model. Chen (1995) tested five different $k-\varepsilon$ models for natural convection, forced convection, mixed convection, and impinging jet in a room. Chen found that it is very difficult to identify any other model superior to the standard $k-\varepsilon$ model. Many studies confirmed applicability of the $k-\varepsilon$ model for thermal comfort and indoor air quality. However, there are many factors that influence the results such as mesh generation, convergence procedure, and boundary condition implementation. Therefore, a more powerful computer and a skilful user are necessary for an effective and accurate simulation.

Realizable $k-\varepsilon$ model [Shih, 1995] was applied with the second order upwind discretization scheme in combination with the standard wall function. The Realizable $k-\varepsilon$ model is a fairly recent addition to the group of two-equation models. It differs from the standard $k-\varepsilon$ model in two ways. First is the turbulent viscosity is computed in a different manner using a variable for the quantity C_μ . This is motivated by the fact that in the limit of highly strained flow, some of the normal Reynolds stresses can become negative in the $k-\varepsilon$ formulation, which is unphysical, or un-realizable. The variable form of the constant C_μ is a function of rotation of the fluid and local strain rate, and is designed to prevent unphysical values of the normal stresses from developing. Secondly, the Realizable $k-\varepsilon$ model uses different sink and source terms in the transport equation for eddy dissipation. The resulting equation is significantly different from the one used for standard and RNG $k-\varepsilon$ models (RNG-based $k-\varepsilon$ turbulence model is derived from the uses mathematical technique called "renormalization group" and is derived from navier strokes equation). The modified prediction of ε , along with the modified calculation for μ_t , makes this turbulence model superior to the other $k-\varepsilon$ models for many applications.

In the present simulation Reynolds number varies from 3000 to 18000. The flow problem in the present case was not subjected to severe pressure gradients and non-equilibrium; therefore, use of standard wall function gives accurate results.

Based upon the above fact that k- ϵ model is most suitable for thermal comfort and indoor air quality analyses, in this CFD analysis Realizable k- ϵ model has been used for analysing the air flow inside the duct of SAH system.

Fluctuations in the velocity field mix transported quantities such as momentum and energy and cause the transported quantities to fluctuate as well. These fluctuations can be of a very

small scale and therefore can create extremely large computational expenses for practical engineering calculations. A modified set of equations that require much less computational expense are used. This is done by time-averaging the instantaneous governing equations which then contain additional unknown variables.

4.3.4 Convergence criteria

To reach convergence, residuals were monitored for the X, Y and Z velocity; continuity; energy; turbulent kinetic energy (k); kinetic energy dissipation rate. The convergence criterion for all the variables is 10^{-3} , except energy whose convergence criterion is 10^{-6} . The solution got converged at the maximum of 400 iterations for steady state operating conditions.

4.3.5 Input parameters

► Materials

Thermo-physical properties including density, thermal conductivity and specific heat capacity of the materials, used for CFD simulation of EATHE are shown in table 4. Flow operating parameters used in the present CFD simulation are velocity and temperature of air at inlet, inlet turbulence intensity and hydraulic diameter.

Table 4.1 Physical and thermal properties of materials used in simulation

Parameter	Material		
	Air	Soil	PVC
Density (kg m ⁻³)	1.225	2050	1380
Specific heat capacity (J kg ⁻¹ K ⁻¹)	1006	1840	900
Thermal conductivity (W m ⁻¹ K ⁻¹)	0.0242	0.52	0.19

Table 4.2 Physical and thermal properties of soil with different moisture content used in simulation

	Dry soil	5 % moisture soil	10 % moisture soil	15 % moisture soil	18 % moisture soil
Density (kg m ⁻³)	2050	2152.5	2255	2357.5	2421
Specific heat capacity (J kg ⁻¹ K ⁻¹)	1840	1785	1719	1657	1624
Thermal conductivity (W m ⁻¹ K ⁻¹)	0.52	0.74	0.9179	1.325	1.61

► Boundary Conditions

In this section, the type of boundary condition for each of the physical boundaries of the EATHE domain is explained.

a. Inlet Conditions

Velocity inlet has been specified at the inlet of EATHE system. Velocity of air inside a pipe i.e 5 m/s was taken as constant for EATHE system and gravity effect is also considered by providing -9.81 m/s in y-axis. To validate simulation result with the experimental three different time intervals are used. Simulation was done for 1hour, 3hour and 11hour operation. In simple(dry) tunnel inlet temperature for 1hour operation is 312.2 K , for 6 hour operation it is 318.5 K while for 11 hour operation it is 311.2 K.

b. Exit Section of Duct

The outlet type “Pressure outlet” was specified on all models and turbulent intensity and hydraulic diameter are same as of inlet section.

c. Walls

Heating plate (absorber) is given uniform heat flux of 1000 W/m^2 and it is assumed that other side walls of inlet section, test section, and outlet section are completely insulated.

d. Other Walls

Walls of the entrance section, exit section and walls of test section other than absorber plate are assumed to be perfectly insulated (wood) and are given 0 W/m^2 radiation intensity.

4.3.6 Grid independence test

As per the practice, grid independence tests are to be conducted to assess the quality of developed CFD model. If the mesh is refined (i.e. the cells are made smaller in size hence larger in number), then the behaviour observed by the post processing should remain unchanged if the solution is grid-independent. In the present analysis, CFD simulations have been performed using a structured grid. Sizing of every edge is done independently.

Refinement of mesh is done by dividing edge in smaller parts and by course and fine meshing method in global mesh settings. A grid-independency test was carried out to check the effect of mesh size on the accuracy of the solution.

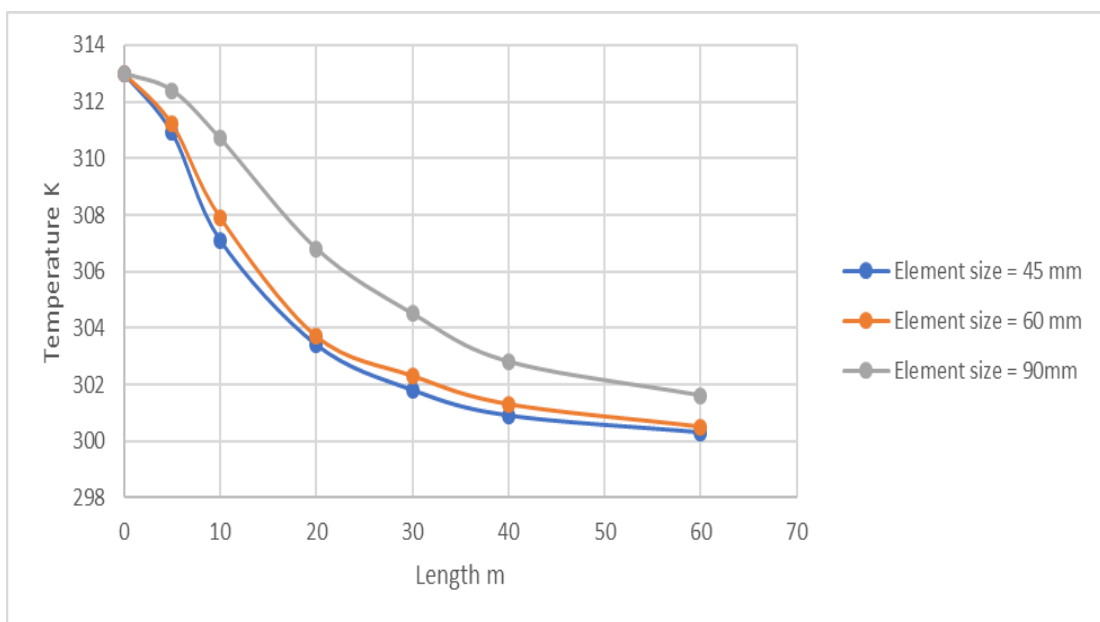


Fig. 4.4 Temperature vs Length for different element size as a result of grid independence test

The independent grid size was determined by successive refinements, grid independent test is carried out for EATHE system by increasing the number of elements by decreasing grid size. Fig. 4.5 shows the simulated value of temperature of air at different length in pipe. Simulation is done on different element sizes varies from 45mm to 90mm and we choose 60mm element size as computational time increases very swiftly. For grid size 60mm no. of nodes and no. of elements are obtained 718675 and 654838 respectively.

Chapter 5

Results and discussion

It has been observed from the previous studies that when hot fluid (in our case air) passes through the pipe buried under the soil, it loses its heat to the surrounding soil. The water(moisture) content present in the soil get evaporates and soil become dry which increase thermal resistance, results in decrease in heat transfer. To study the problem of soil saturation we developed the 4 different models of EATHE system i.e. dry soil, soil with 5% moisture content, soil with 10% moisture content and soil with 15% moisture content. We simulated the model for three different time intervals i.e. 1 hour, 6 hours and 11 hours operation for each case and compare the results with the experimental.

5.1 Performance analysis of dry EATHE systems for summer cooling

Variation in temperature of air along the length of pipes of dry EATHE systems at a flow velocity of 5 m/s was analysed for different time interval and their simulation results were compared with secondary experimental results.

5.1.1 Results of dry soil simulation of 1 hour operation

Dry soil having thermal conductivity 0.52 W/ m-K is used to heat transfer with incoming air at temperature 312.2 K. Temperature is measured at different length of pipe and compare the results with the experimental as shown in figure 5.1. There is a slight difference between the outlet temperature of experiment and simulated result, in term of error % it is 1.327%.

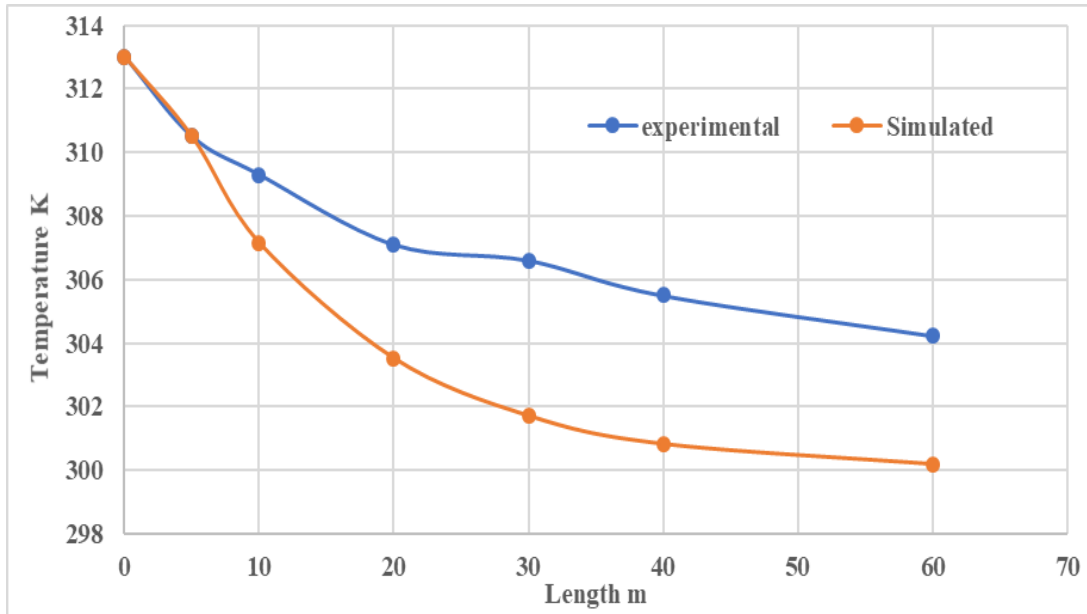


Figure 5.1 Variation of Temperature with length of dry soil for 1 hour operation

5.1.2 Results of dry soil simulation of 6 hours operation

Dry soil having thermal conductivity 0.52 W/ m-K is used to heat transfer with incoming air at temperature 318.5 K . Temperature is measured at different length of pipe and compare the results with the experimental as shown in figure 5.2. There is a slight difference between the outlet temperature of experiment and simulated result, in term of error % it is 1.05% .

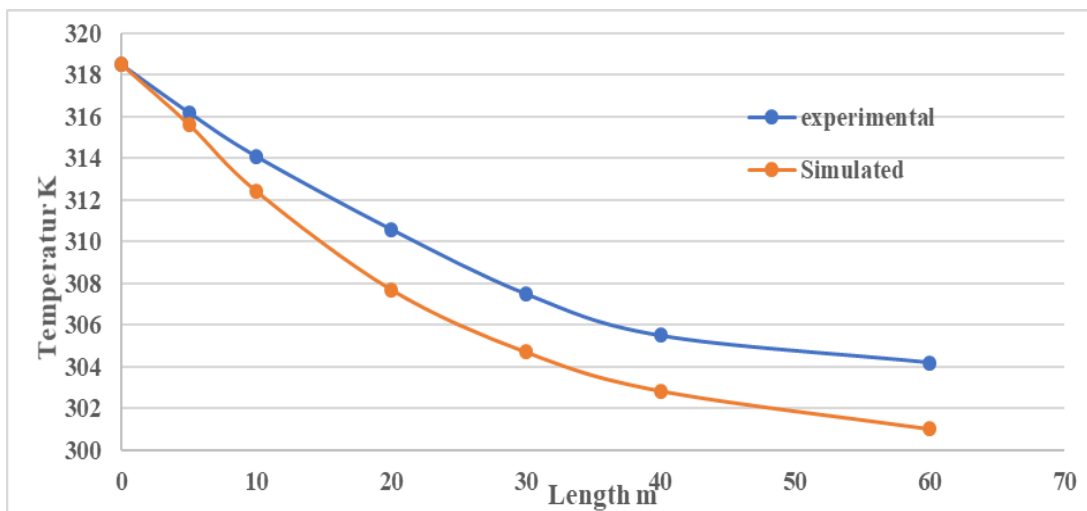


Figure 5.2 Variation of Temperature with length of dry soil for 6 hours operation

5.1.3 Results of dry soil simulation of 11 hours operation

Dry soil having thermal conductivity 0.52 W/ m-K is used to heat transfer with incoming air at temperature 311.6 K . Temperature is measured at different length of pipe and compare the results with the experimental as shown in figure 5.3. There is a slight difference between the outlet temperature of experiment and simulated result, in term of error % it is 1.08% .

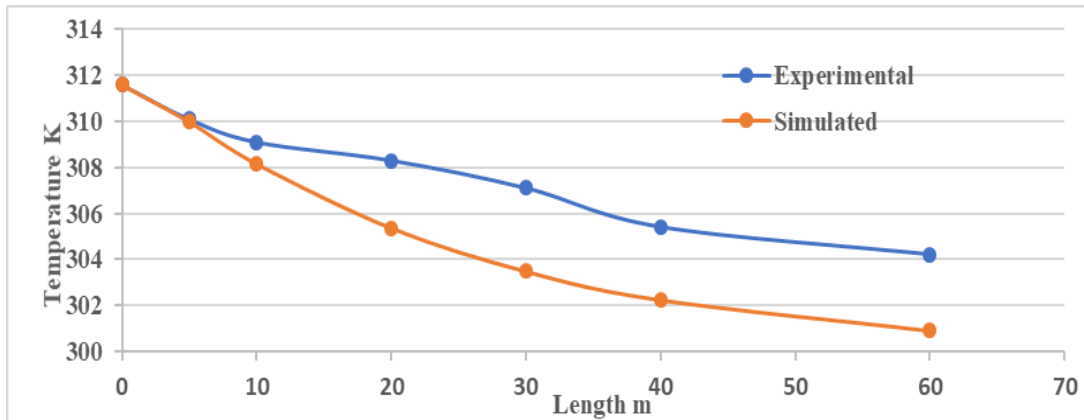


Figure 5.3 Variation of Temperature with length of dry soil for 11 hours operation

5.2 Performance analysis of wet EATHE systems with 5% moisture content for summer cooling

Variation in temperature of air along the length of pipes of wet EATHE systems with 5% moisture content at a flow velocity of 5 m/s was analysed for different time interval and their simulation results were compared with secondary experimental results.

5.2.1 Results of soil with 5% moisture content simulation of 1 hour operation

Soil with 5% moisture content having thermal conductivity 0.74 W/ m-K is used to heat transfer with incoming air at temperature 312.2 K . Temperature is measured at different length of pipe and compare the results with the experimental as shown in figure 5.4. There is a slight difference between the outlet temperature of experiment and simulated result, in term of error % it is 1.18% .

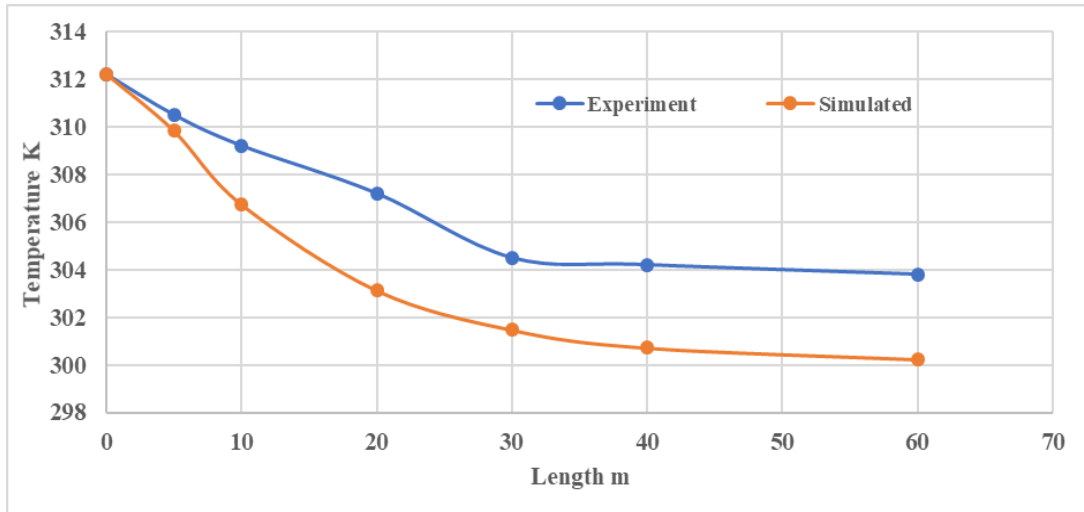


Figure 5.4 Variation of Temperature with length of soil with 5% moisture for 1 hours operation

5.2.2 Results of soil with 5% moisture content simulation of 6 hours operation

Soil with 5% moisture content having thermal conductivity 0.74 W/ m-K is used to heat transfer with incoming air at temperature 318.5 K.

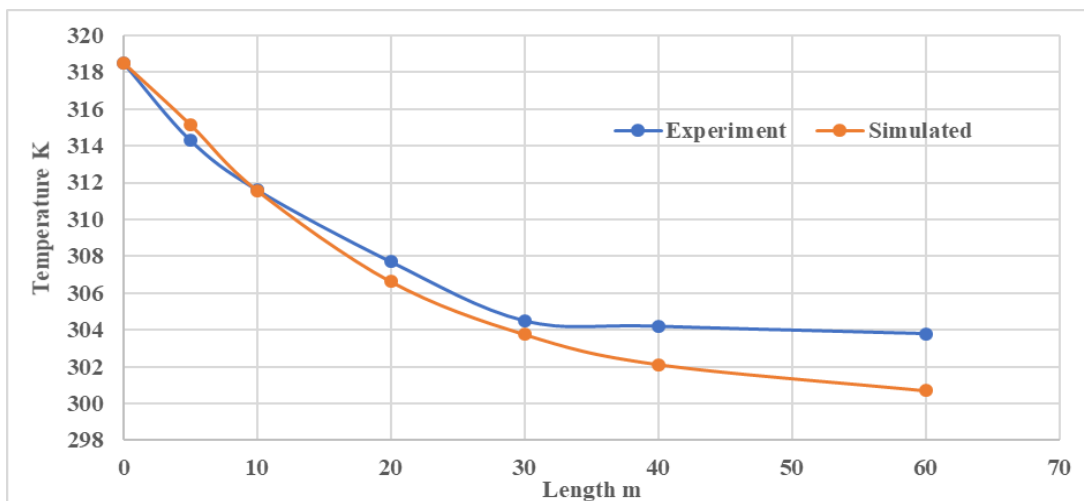


Figure 5.5 Variation of Temperature with length of soil with 5% moisture for 6 hours operation

Temperature is measured at different length of pipe and compare the results with the experimental as shown in figure 5.5. There is a slight difference between the outlet temperature of experiment and simulated result, in term of error % it is 1.05%

5.2.3 Results of soil with 5% moisture content simulation of 11 hours operation

Soil with 5% moisture content having thermal conductivity 0.74 W/ m-K is used to heat transfer with incoming air at temperature 311.6 K. Temperature is measured at different length of pipe and compare the results with the experimental as shown in figure 5.6. There is a slight difference between the outlet temperature of experiment and simulated result, in term of error % it is 1.08%

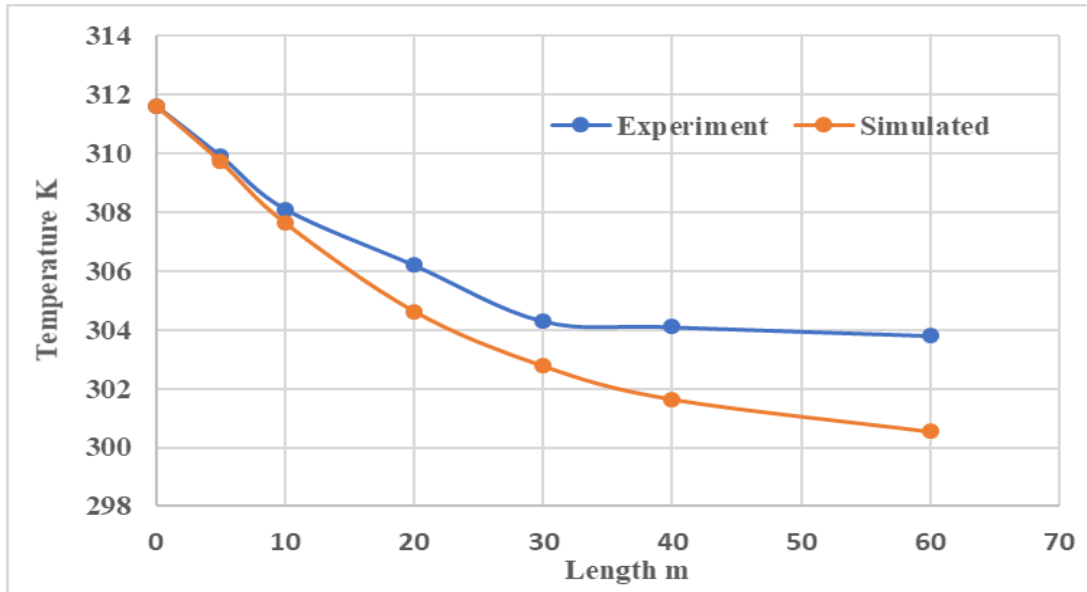


Figure 5.6 Variation of Temperature with length of soil with 5% moisture for 11 hours operation

5.3 Performance analysis of wet EATHE systems with 10% moisture content for summer cooling

Variation in temperature of air along the length of pipes of wet EATHE systems with 5% moisture content at a flow velocity of 2 m/s was analysed for different time interval and their simulation results were compared with secondary experimental results.

5.3.1 Results of soil with 10% moisture content simulation of 1 hour operation

Soil with 10% moisture content having thermal conductivity 0.9179 W/ m-K is used to heat transfer with incoming air at temperature 311.9 K. Temperature is measured at different length of pipe and compare the results with the experimental as shown in figure 5.7. There is a slight difference between the outlet temperature of experiment and simulated result, in term of error % it is 1.18%

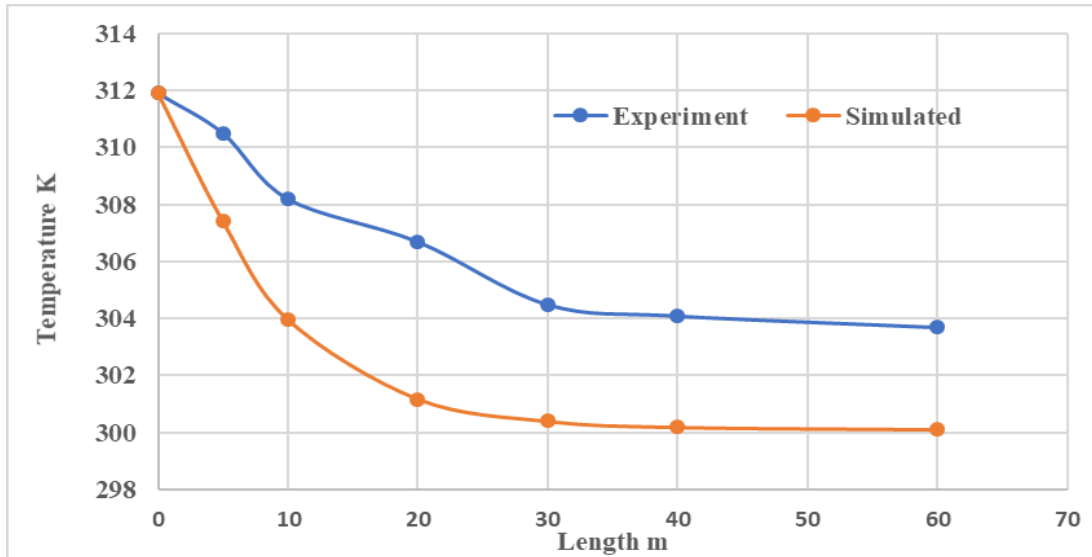


Figure 5.7 Variation of Temperature with length of soil with 10% moisture for 1 hours operation

5.3.2 Results of soil with 10% moisture content simulation of 6 hours operation

Soil with 10% moisture content having thermal conductivity 0.9179 W/ m-K is used to heat transfer with incoming air at temperature 318.5 K. Temperature is measured at different length of pipe and compare the results with the experimental as shown in figure 5.8. There is a slight difference between the outlet temperature of experiment and simulated result, in term of error % it is 1.15%

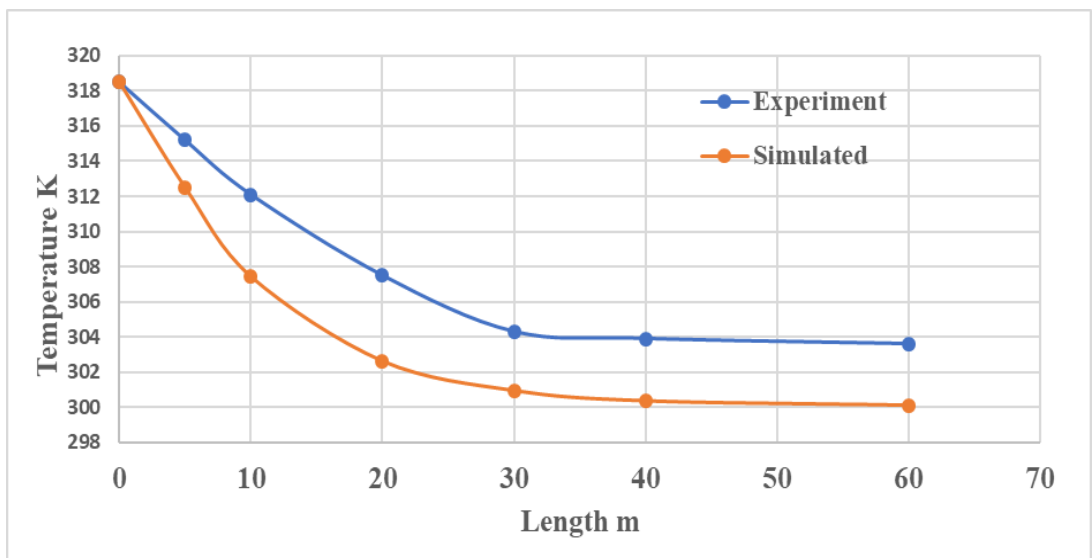


Figure 5.8 Variation of Temperature with length of soil with 10% moisture for 6 hours operation

5.3.3 Results of soil with 10% moisture content simulation of 11 hours operation

Soil with 10% moisture content having thermal conductivity 0.9179 W/ m-K is used to heat transfer with incoming air at temperature 312.1 K. Temperature is measured at different length of pipe and compare the results with the experimental as shown in figure 5.9. There is a slight difference between the outlet temperature of experiment and simulated result, in term of error % it is 1.15%

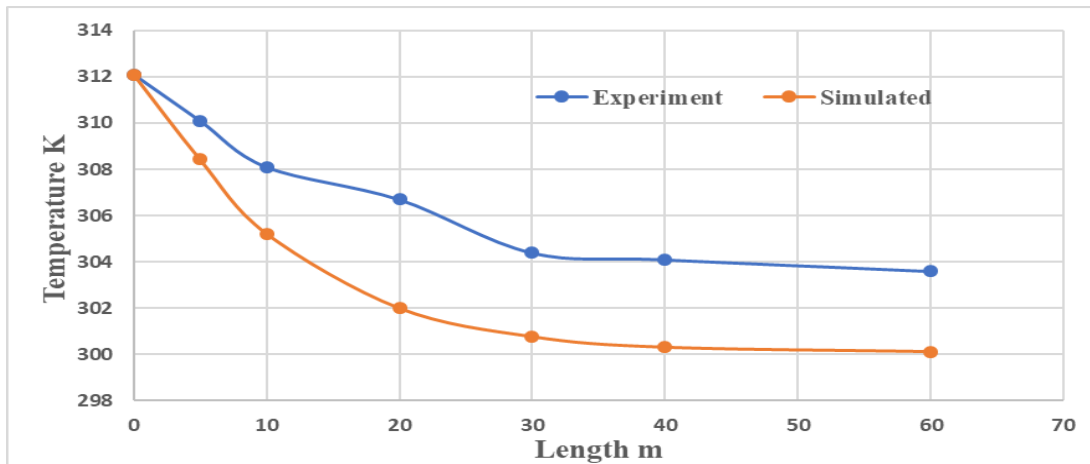


Figure 5.9 Variation of Temperature with length of soil with 10% moisture for 11 hours operation

5.4 Performance analysis of wet EATHE systems with 15% moisture content for summer cooling

Variation in temperature of air along the length of pipes of wet EATHE systems with 5% moisture content at a flow velocity of 2 m/s was analysed for different time interval and their simulation results were compared with secondary experimental results.

5.4.1 Results of soil with 15% moisture content simulation of 1 hour operation

Soil with 15% moisture content having thermal conductivity 1.22 W/ m-K is used to heat transfer with incoming air at temperature 311.7 K.

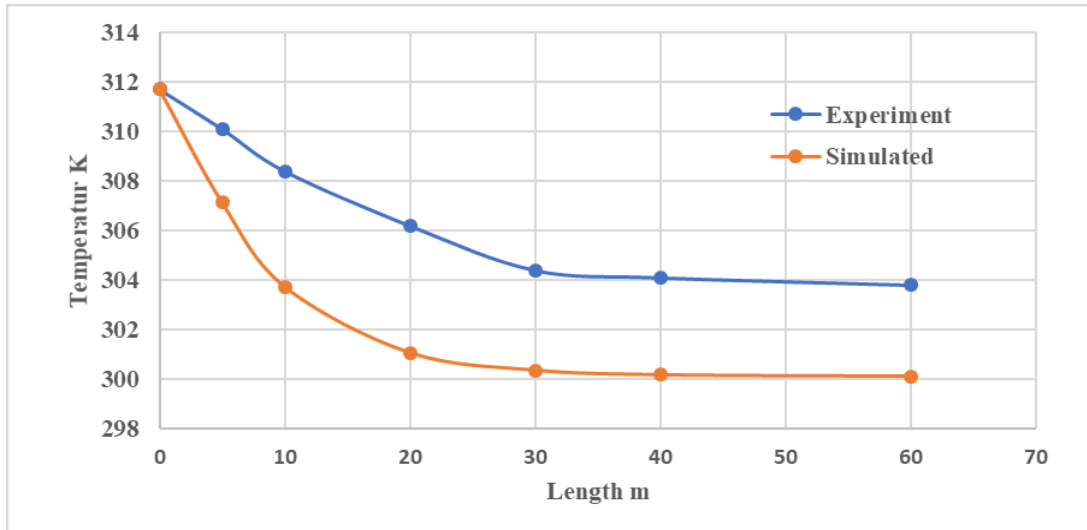


Figure 5.10 Variation of Temperature with length of soil with 15% moisture for 1 hour operation

Temperature is measured at different length of pipe and compare the results with the experimental as shown in figure 5.10. There is a slight difference between the outlet temperature of experiment and simulated result, in term of error % it is 1.21%

5.4.2 Results of soil with 15% moisture content simulation of 6 hours operation

Soil with 15% moisture content having thermal conductivity 1.22 W/ m-K is used to heat transfer with incoming air at temperature 318.5 K. Temperature is measured at different length of pipe and compare the results with the experimental as shown in figure 5.11. There is a slight difference between the outlet temperature of experiment and simulated result, in term of error % it is 1.15%

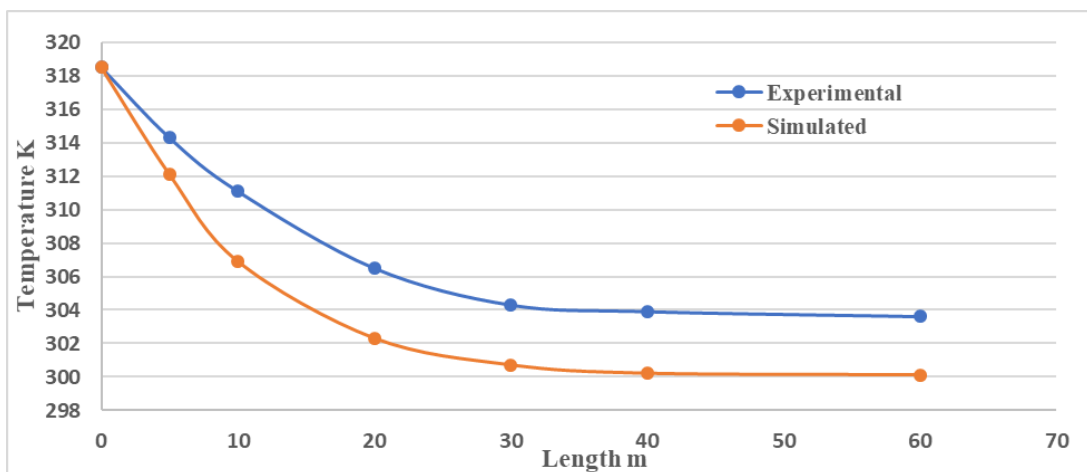


Figure 5.11 Variation of Temperature with length of soil with 15% moisture for 6 hours operation

5.4.3 Results of soil with 15% moisture content simulation of 11 hours operation

Soil with 15% moisture content having thermal conductivity 1.22 W/ m-K is used to heat transfer with incoming air at temperature 311.6 K. Temperature is measured at different length of pipe and compare the results with the experimental as shown in figure 5.12. There is a slight difference between the outlet temperature of experiment and simulated result, in term of error % it is 1.21 %

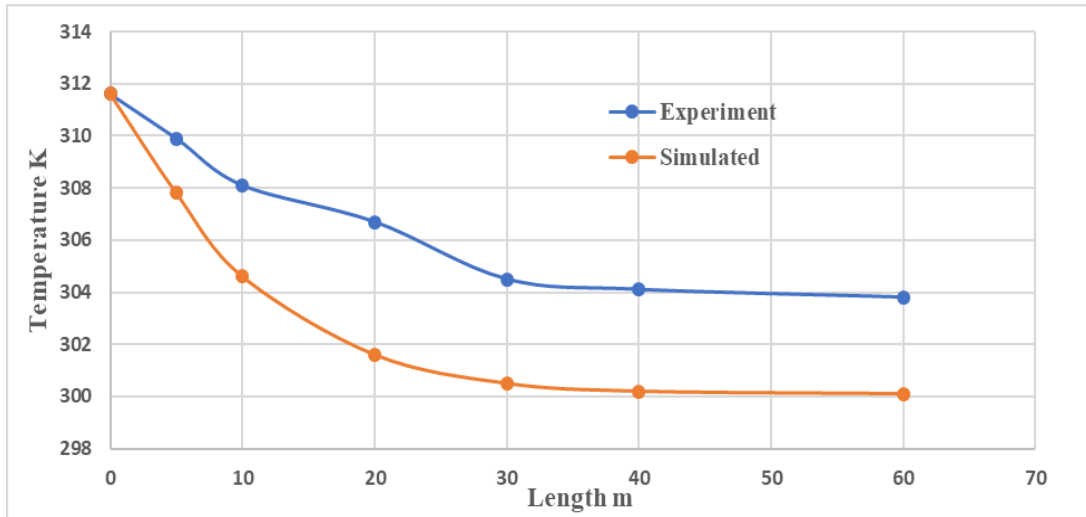


Figure 5.12 Variation of Temperature with length of soil with 15% moisture for 11 hours operation

Here an important term coined as *Knee Point* is being introduced. *Position of knee point reflects the length of the EATHE pipe at which 90% of total drop in air temperature is obtained.* Beyond Knee point an appreciable drop in air temperature is not observed. From Figure 5.1 to Figure 5.3 knee point comes out to be 41 m, 42 m and 45 m respectively. It is noticed that as the time of operation increased from 1 hour to 11 hours knee point increases as soil start saturating and more length needed for same temperature drop. In wet system (5% moisture content) the pipe length at which 90% of total temperature drop is obtained, lies at 30 m, 34 m, 40 m for 1 hour, 6 hours and 11 hours of operation respectively. For 10% moisture content, the pipe length at which 90% of total temperature drop is obtained, lies at 22 m, 25 m, 27 m for 1 hour, 6 hours and 11 hours of operation respectively. For 15% moisture content, the pipe length at which 90% of total temperature drop is obtained, lies at 20 m, 21 m, 23 m for 1 hour, 6 hours and 11 hours of operation respectively. Therefore, the behaviour of soil changes due to the presence of moisture tremendously and it diffuses most of

the heat to surrounding soil layers at a faster rate. Therefore, the presence of moisture greatly affects the length of EATHE pipe required to achieve a specified temperature drop. From Figure 5.1 to Figure 5.12 it is observed that a significantly shorter length of EATHE pipe (28m) is sufficient to provide 90% of the total temperature drop.

It is being observed from figure 5.1 to 5.12, as we keep on increasing the moisture content thermal conductivity of the soil keep on increasing and knee length decrease but simulation results of 18% moisture content for 1 hour operation shows no significant decrease in knee length as shown in figure 5.13.

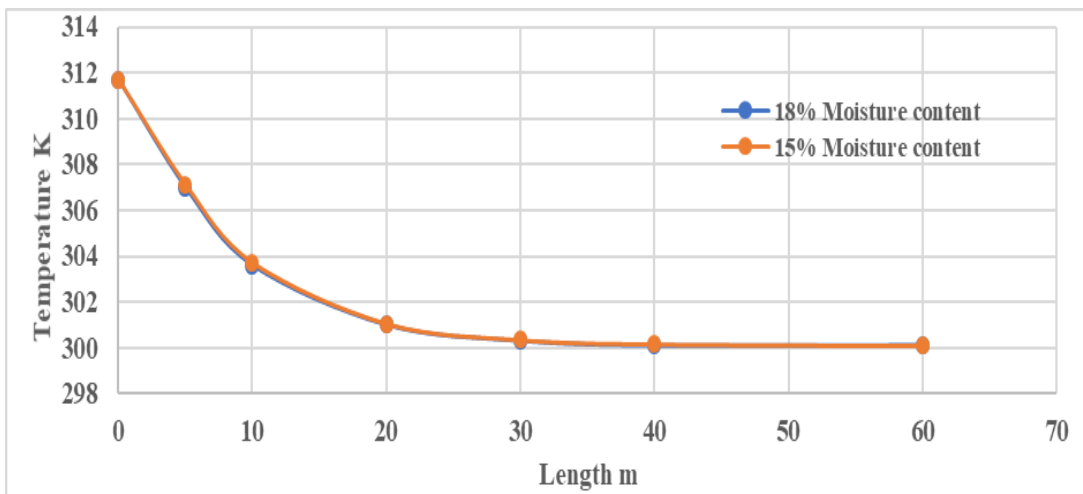


Figure 5.13 Variation of Temperature with length of soil with 15% and 18% moisture for 1 hours operation

5.5 U-Shaped geometry results

U-shaped geometry of EATHE has been developed in both Auto-cad and ANSYS fluent 15.0 with the same dimension as that in experiment done by Dharmendra Kumar saini is shown in figure 5.14. 5.15 respectively.

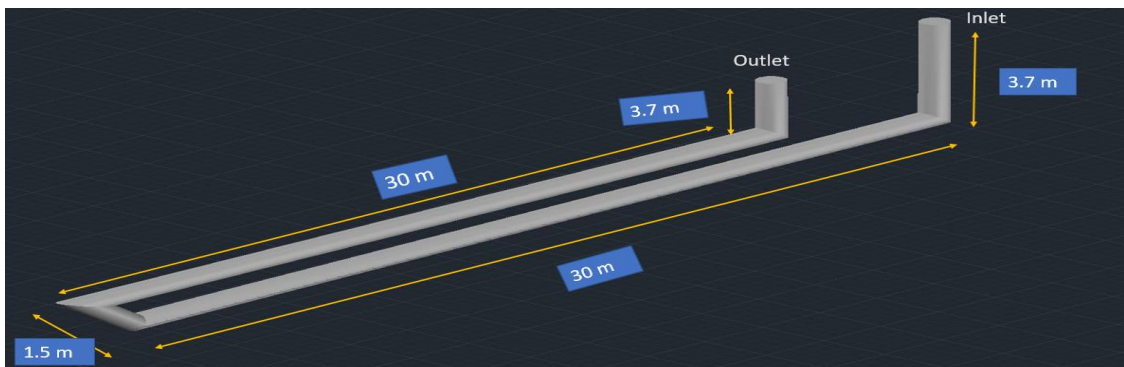


Figure 5.14 Auto-cad geometry of U-Shaped EATHE

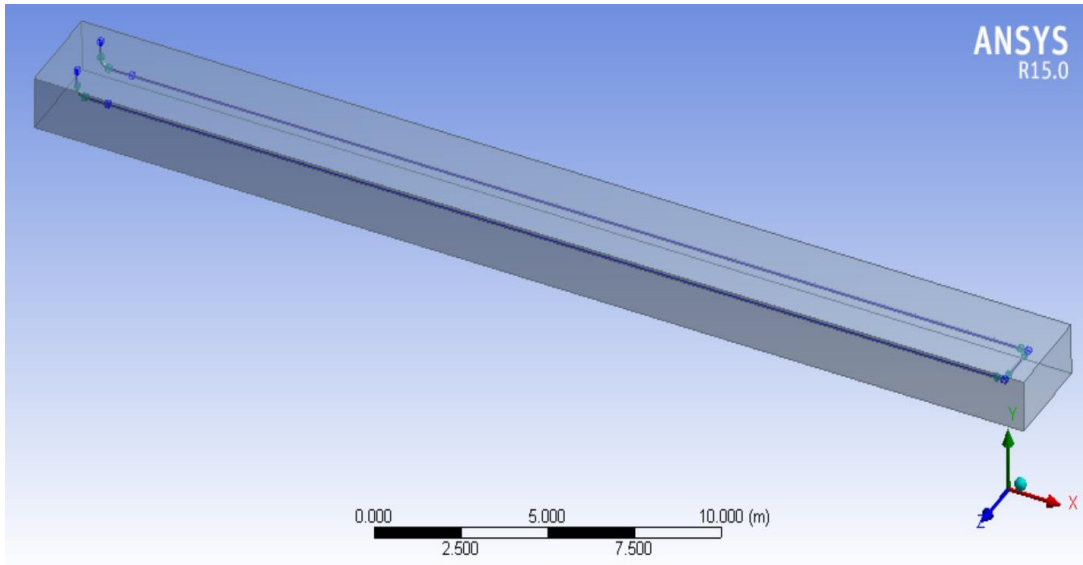


Figure 5.15 Ansys fluent geometry of U-Shaped EATHE

5.5.1 Comparison of straight shaped and U-shaped pipe geometry for dry soil 1 hour operation

Dry soil having thermal conductivity 0.52 W/ m-K is used to heat transfer with incoming air at temperature 313 K. Temperature is measured at different length of pipe and compare the results with the experimental as shown in figure 5.16. There is a slight difference between the maximum temperature of Straight shaped and U-shaped pipe geometry result, in term of error % it is 0.65%.

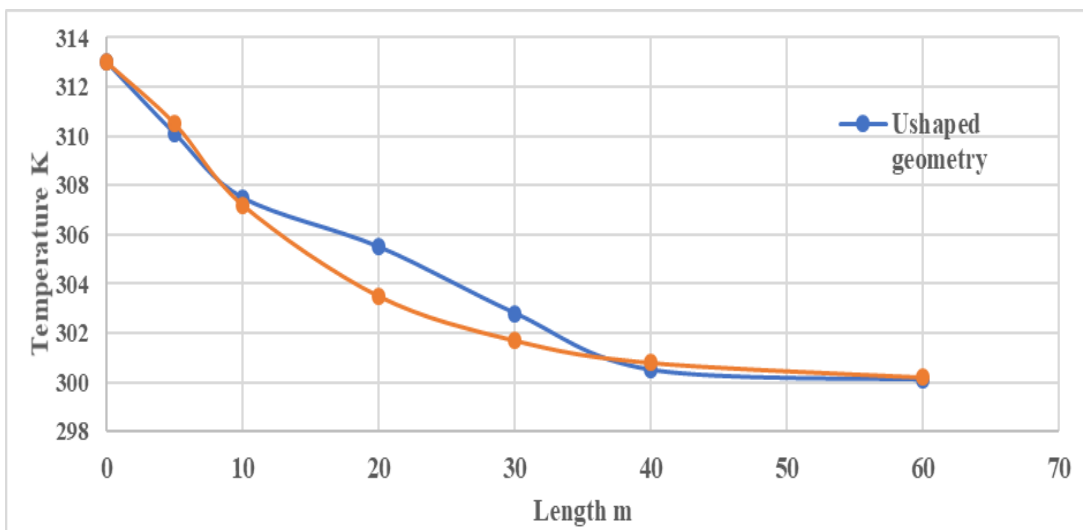


Figure 5.16 Variation of straight shaped vs U-shaped geometry of dry soil for 1 hours operation

5.5.2 Comparison of straight shaped and U-shaped pipe geometry soil with 5% moisture content for 1 hour operation

Soil having thermal conductivity 0.74 W/ m-K is used to heat transfer with incoming air at temperature 312.2 K. Temperature is measured at different length of pipe and compare the results with the experimental as shown in figure 5.17. There is a slight difference between the maximum temperature of Straight shaped and U-shaped pipe geometry result, in term of error % it is 0.29%.

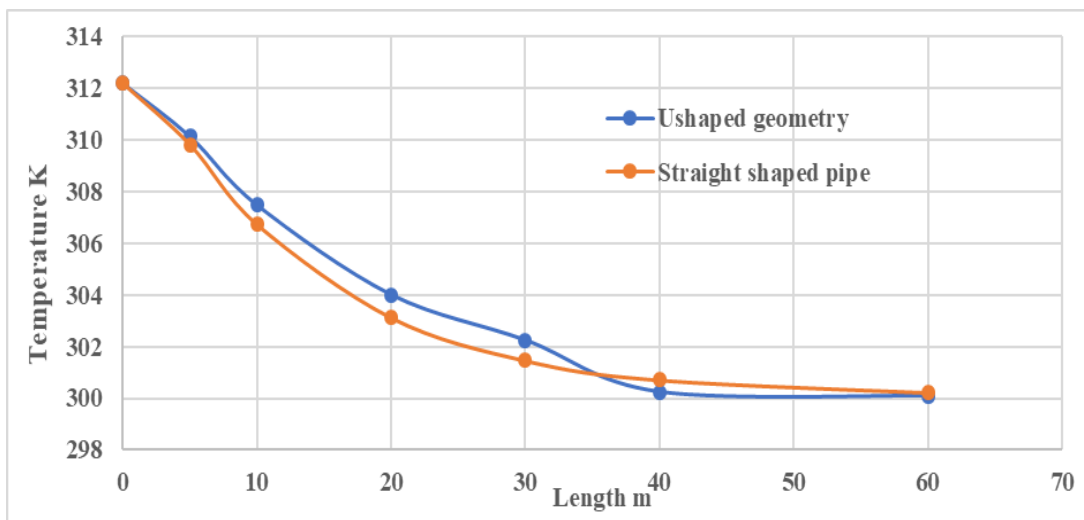


Figure 5.17 Variation of straight shaped vs U-shaped geometry of soil with 5% moisture content for 1 hours operation

5.5.3 Comparison of straight shaped and U-shaped pipe geometry soil with 10% moisture content for 1 hour operation

Soil having thermal conductivity 0.9179 W/ m-K is used to heat transfer with incoming air at temperature 311.9 K. Temperature is measured at different length of pipe and compare the results with the experimental as shown in figure 5.18. There is a slight difference between the maximum temperature of Straight shaped and U-shaped pipe geometry result, in term of error % it is 0.055%.

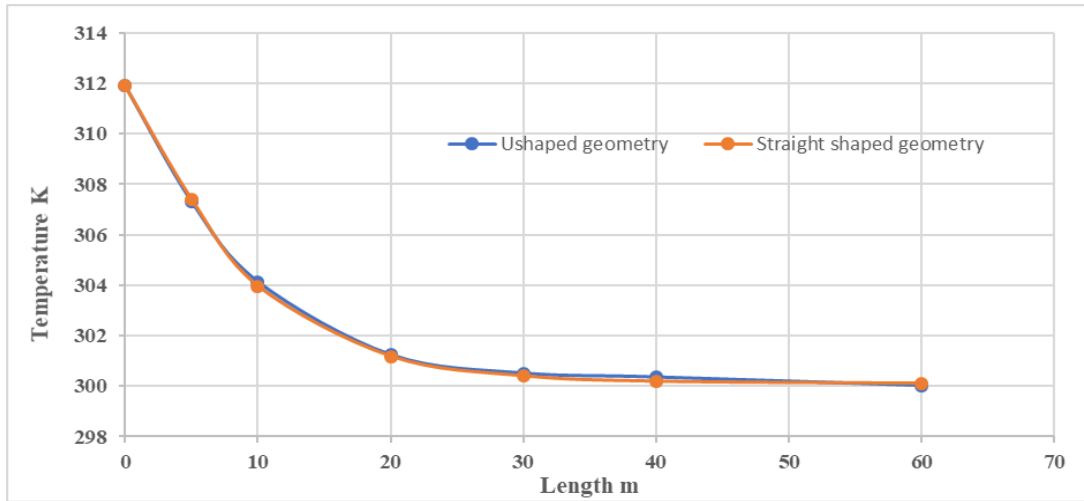


Figure 5.18 Variation of straight shaped vs U-shaped geometry of soil with 10% moisture content for 1 hours operation

5.5.4 Comparison of straight shaped and U-shaped pipe geometry soil with 15% moisture content for 1 hour operation

Soil having thermal conductivity 1.22 W/ m-K is used to heat transfer with incoming air at temperature 311.7 K. Temperature is measured at different length of pipe and compare the results with the experimental as shown in figure 5.19. There is a slight difference between the maximum temperature of Straight shaped and U-shaped pipe geometry result, in term of error % it is 0.04%.

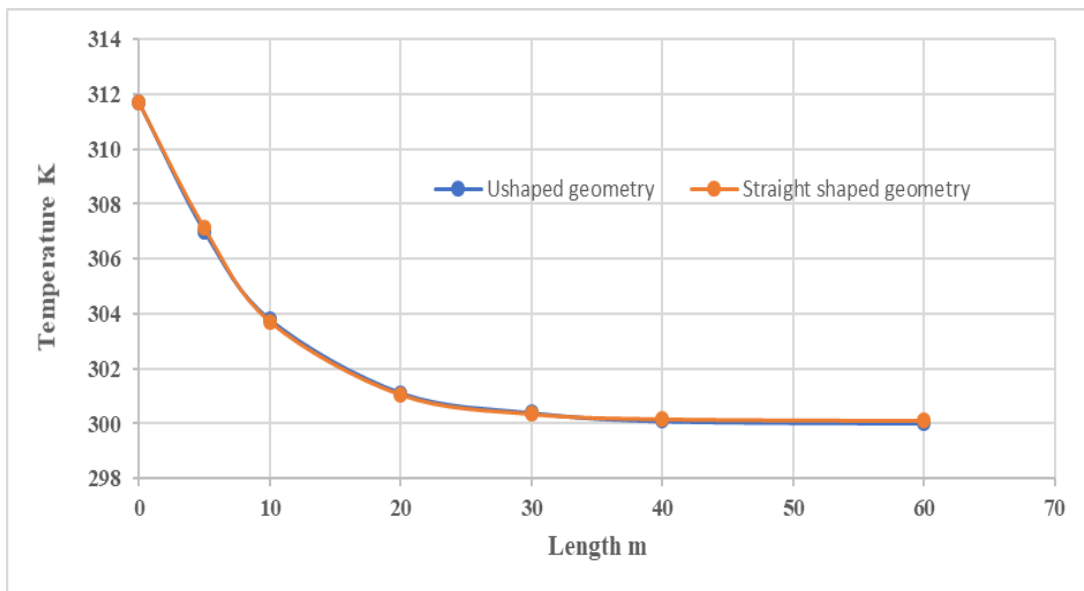


Figure 5.19 Variation of straight shaped vs U-shaped geometry of soil with 15% moisture content for 1 hours operation

5.5.5 Comparison of straight shaped and U-shaped pipe geometry soil with 15% moisture content for 6 hours operation

Soil having thermal conductivity 1.22 W/ m-K is used to heat transfer with incoming air at temperature 318.5 K. Temperature is measured at different length of pipe and compare the results with the experimental as shown in figure 5.20. There is a slight difference between the maximum temperature of Straight shaped and U-shaped pipe geometry result, in term of error % it is 0.22%.

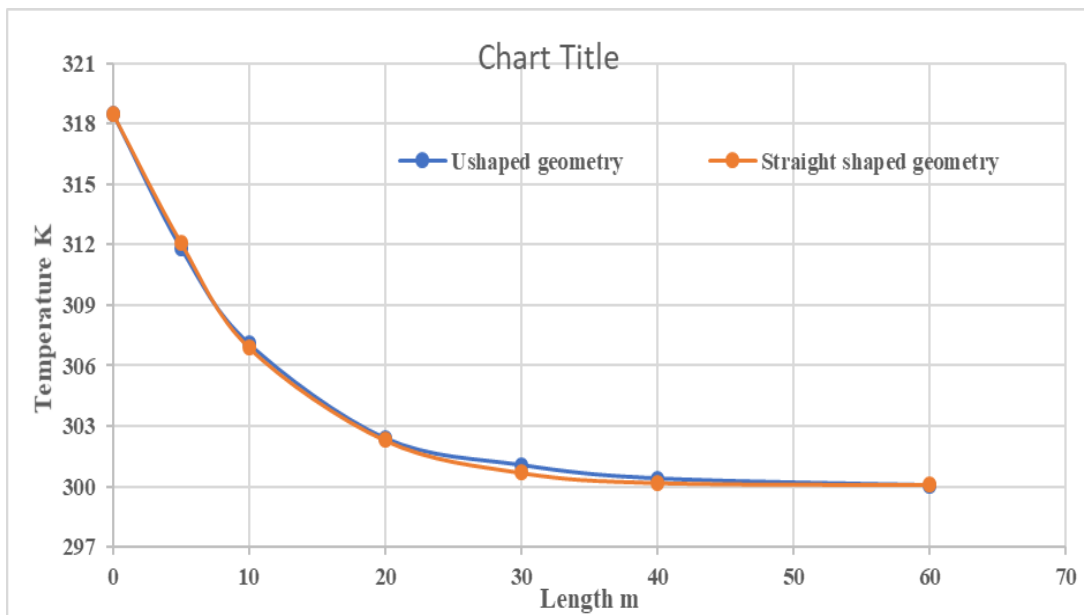


Figure 5.20 Variation of straight shaped vs U-shaped geometry of soil with 15% moisture content for 6 hours operation

5.5.6 Comparison of straight shaped and U-shaped pipe geometry soil with 15% moisture content for 11 hours operation

Soil having thermal conductivity 1.22 W/ m-K is used to heat transfer with incoming air at temperature 311.6 K. Temperature is measured at different length of pipe and compare the results with the experimental as shown in figure 5.21. There is a slight difference between the maximum temperature of Straight shaped and U-shaped pipe geometry result, in term of error % it is 0.12%.

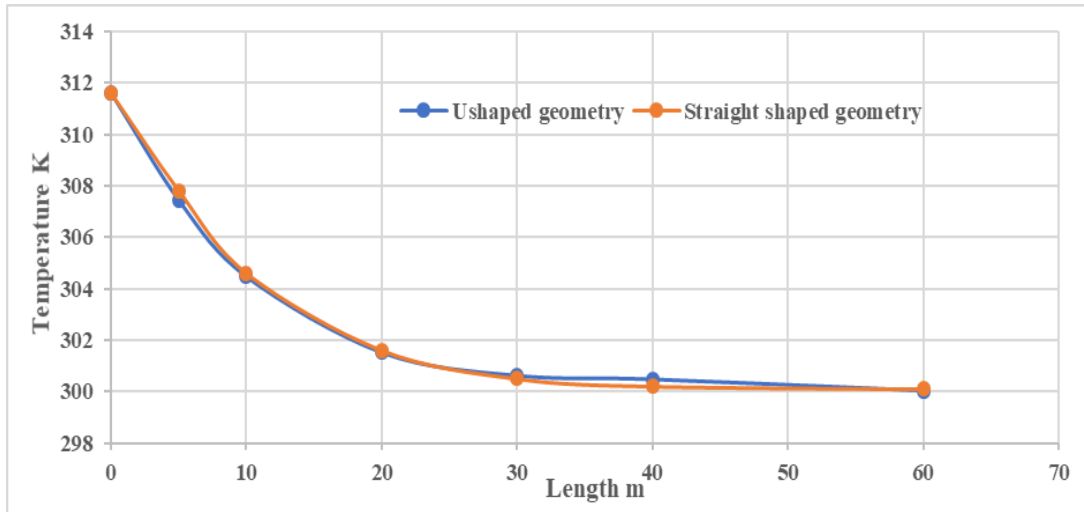


Figure 5.21 Variation of straight shaped vs U-shaped geometry of soil with 15% moisture content for 11 hours operation

5.6 Velocity variation of the EATHE system

Inlet velocity of air was taken 5 m/s in our study but for dry soil one hour operation different velocity variation was also studied. Three different velocity i.e. 2m/s, 4m/s and 6m/s was simulated for dry soil one hour operation as shown in figure 5.22. It was observed from the figure that as we keep on increasing the velocity of incoming air the heat transfer rate keep on decreasing and incoming air will needed longer pipe to cool. Hence larger the velocity, larger the knee length.

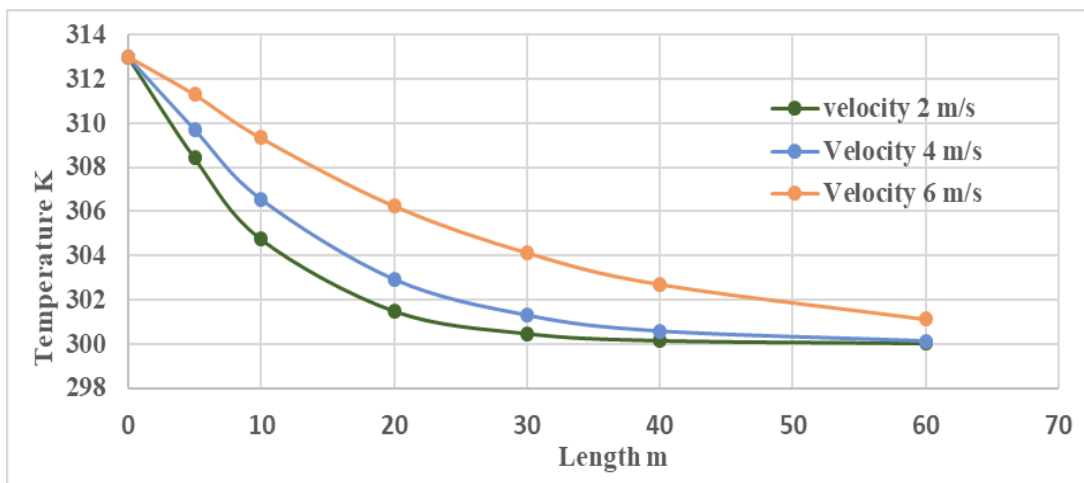


Figure 5.22 Velocity variation of dry soil one hour operation of EATHE system

Chapter 6

Conclusion

EATHE has some inherent limitations in real application due to the soil thermal saturation especially in low thermal conductivity soil. To increase the thermal conductivity of soil, four different operation modes namely dry soil, wet soil with 5% moisture content, wet soil with 10% moisture content and wet soil with 15% moisture content have been analysed also the different velocity variation has been observed. In the present work, a numerical simulation model of EATHE system has been modelled and validated with the existing experimental facility. The following conclusions can be obtained:

1. In the first mode of operation, dry soil with soil thermal conductivity 0.52 W/m-K is simulated for three different time interval i.e 1 hour, 6 hours and 11 hours. Simulated results for each time interval is compared and validate with experimental results. The knee length for 1 hour, 6 hours and 11 hours of operation comes out to be 41m, 42m and 45m respectively.
2. In the second mode of operation, wet soil of 5% moisture content having soil thermal conductivity 0.74 W/m-K is simulated for three different time intervals i.e. 1 hour, 6 hours and 11 hours. Simulated results for each time interval is compared and validate with experimental results. The knee length for 1 hour, 6 hours and 11 hours of operation comes out to be 30 m, 34 m and 40 m respectively.
3. In the third mode of operation, wet soil of 10% moisture content having soil thermal conductivity 0.917 W/m-K is simulated for three different time intervals i.e. 1 hour, 6 hours and 11 hours. Simulated results for each time interval is compared and validate with experimental results. The knee length for 1 hour, 6 hours and 11 hours of operation comes out to be 22 m, 25 m and 27 m respectively.
4. In the fourth mode of operation, wet soil of 15% moisture content having soil thermal conductivity 1.22 W/m-K is simulated for three different time intervals i.e. 1 hour, 6 hours and 11 hours. Simulated results for each time

interval is compared and validate with experimental results. The knee length for 1 hour, 6 hours and 11 hours of operation comes out to be 20 m, 21 m and 23 m respectively.

5. In the fifth mode of operation, wet soil of 18% moisture content having soil thermal conductivity 1.61 W/m-K is simulated for 1 hour and compared with soil having 15% moisture content. It has been observed that simulated results for 15% and 18% moisture content soil have almost same results. Hence no significant increase in heat transfer rate for 18% moisture content.

Different velocity variation of dry soil for one hour operation was also studied. Three different velocity i.e. 2m/s, 4m/s and 6m/s was simulated. It was observed from the results that as we keep on increasing the velocity of incoming air the heat transfer rate keep on decreasing and incoming air will needed longer pipe to cool. Hence larger the velocity of incoming air, larger the knee length.

6.1 Scope for Future work

A lot of study on EATHE system has been done by many researchers till now. This study is also helps to extend the research work on EATHE system, but still there is a lot of scope of further study.

1. One of the scopes of further study is to develop the correlation for the soil thermal diffusivity, length of pipe, diameter of pipe, and velocity of air in transient conditions.
2. Dynamic night purging according to the ambient temperature and varying air flow rate.
3. Less study has been done on comparison of steady and transient work.
4. Need more studies on Derating factor.

References

- [1] Trombe A., Pettit M., B. Bourret, “Air cooling by earth tube heat exchanger: experimental approach,” *Renew. Energy*, vol. 1, no. 5–6, pp. 699–707, 1991.
- [2] G. Mihalakakou, M. Santamouris, and D. Asimakopoulos, “Modelling the thermal performance of earth-to-air heat exchangers,” *Sol. energy*, vol. 53, no. 3, pp. 301–305, 1994.
- [3] Kumar R., Sinha A. R., Singh B. K, Modhukalya U., 2008, A design optimization tool of earth-to-air heat exchanger using a genetic algorithm, *Renewable Energy*, Vol. 33, pp. 2282–2288.
- [4] Puri V. M., 1987, Heat and mass transfer analysis and modelling in unsaturated ground soils for buried tube systems, *Energy in Agriculture*, Vol. 6, pp. 179–193.
- [5] R. Kumar, S. Ramesh, and S. C. Kaushik, “Performance evaluation and energy conservation potential of earth–air–tunnel system coupled with non-air-conditioned building,” *Build. Environ.*, vol. 38, no. 6, pp. 807–813, Jun. 2003.
- [6] Tzaferis A., Liparakis D., Santamouris M., Argiriou A., 1992, “Analysis of the accuracy and sensitivity of eight models to predict the performance of earth-to-air heat exchangers”, *Energy and Buildings*, 18(1992)35-43.
- [7] Liu B.C., Liu W., Peng S. W., 2005, Study of heat and moisture transfer in soil with a dry surface layer, *International Journal of Heat and Mass Transfer* 48(2005) 4579–4589.
- [8] Ajmi F. Al., Loveday D. L., Hanby V., “The cooling potential of earth–air heat exchangers for domestic buildings in a desert climate”, *Building and Environment* 41(2006) 235–244.
- [9] Khandelwal, Kumar S., Mathur A., and Agrawal G.D., "The Design of Earth Air Tunnel Heat Exchanger System for an Institute Library." *International Journal of Scientific Engineering and Technology* 43 (2015): 141-145.
- [10] M. Khabbaz, B. Benhamou, K. Limam, P. Hollmuller, H. Hamdi, and A. Bennouna, “Experimental and numerical study of an earth-to-air heat

- exchanger for air cooling in a residential building in hot semi-arid climate,” *Energy Build.* 125(2016) 109–121.
- [11] Sharan G., Jadhav R., 2003, Performance of single pass earth-tube heat exchanger: An experimental study, *Journal of Agricultural Engineering*, Vol. 40(1), pp. 1-8.
- [12] Ozgener L., Ozgener O., 2010, An experimental study of the exergetic performance of an underground air tunnel system for green house cooling, *Renewable Energy*, Vol. 35, pp. 2804–2811.
- [13] Bansal V., Misra R., Mathur J., Agrawal G. D., 2013, Transient effect of soil thermal conductivity and duration of operation on performance of Earth Air Tunnel Heat Exchanger, *Applied Energy*, Vol. 103, pp. 1–11.
- [14] G.-E. Vlad, C. Ionescu, H. Necula, and A. Badea, “Simulation of an air heating/cooling system that uses the ground thermal potential and heat recovery,” *UPB Sci. Bull. Ser. C*, vol. 75, no. 3, pp. 239–246, 2013.
- [15] Singh A. K., Tiwari G. N., Lugani N., Garg H. P., 1996, Energy conservation in a cinema hall under hot and dry condition, *Energy Conversion and Management*, Vol. 37(5), pp. 531-539.
- [16] Benhammou, M. "Performance analysis of an earth-to-air heat exchanger assisted by a wind tower for passive cooling of buildings in arid and hot climate." *Energy Conversion and Management* 91 (2015): 1-11.
- [17] S. Jakhar, R. Misra, M. S. Soni, and N. Gakkhar, “Parametric simulation and experimental analysis of earth air heat exchanger with solar air heating duct,” *Eng. Sci. Technol. an Int. J.*, pp. 1–8, 2016.
- [18] V. Bansal, R. Misra, G. Das Agrawal, and J. Mathur, “Performance analysis of earth–pipe–air heat exchanger for winter heating,” *Energy Build.*, vol. 41, no. 11, pp. 1151–1154, Nov. 2009.
- [19] Bansal V., Mishra R., Agrawal G.D., Mathur J., “Performance evaluation and economic analysis of integrated earth-air-tunnel heat exchanger-evaporative cooling system”, *Energy and Buildings* 55(2012) 102-108.

- [20] Ozgener O., Ozener L., “ Determining the optimal design of a closed loop earth to air heat exchanger for greenhouse heating by using exergoeconomics” *Energy and Buildings* 43 (2011) 960-965.
- [21] Mathure A., Srivastava A., Mathur J., Mathur S., “ Transient effect of soil thermal diffusivity on performance of EATHE system” *Energy Reports* 1(2015) 17-21.
- [22] Mathure A., Srivastava A., Agrawal G.D., Mathur S., Mathur J., “CFD analysis of EATHE system under transient conditions for intermittent operation”, *Energy and Buildings* 87(2015) 37-44.
- [23] Mishra R., Agrawal G.D., Mathur J., Bansal V., Aseri T., “ Transient analysis based determination of derating factor for EATHE in winter”, *Energy and Buildings* 58(2013) 76-85.
- [24] Ozgener O., Ozener L., Tester J.W., “A practical approach to predict soil temperature variations for geothermal (ground) heat exchangers applications”, *Int. journal of heat and mass transfer* 62(2013) 473-480.
- [25] Niu F., Yu Y., Yu D., Li H., “Investigation on Soil Thermal Saturation and Recovery of an Earth to Air Heat Exchanger under Different Operation Strategies”, *Applied thermal Engineering* 77(2015) 90-100.

APPENDIX A.1

Turbulence Models

The equations of motion are averaged with respect to time and these turbulent transport models predict the effect of turbulence on the time averaged mean motion. Since all of the terms currently in the equations of motion are instantaneous values, they are replaced with the sum of a time-mean quantity and a fluctuating quantity, with $T =$ the sum of a time-mean quantity and a fluctuating quantity. A new set of equations of motion with the same form are obtained with the addition of these quantities.

Energy

$$\begin{aligned} \frac{\partial}{\partial t}(\rho c_p \bar{T}) + \frac{\partial}{\partial x}(\rho \bar{u} c_p \bar{T}) + \frac{\partial}{\partial y}(\rho \bar{v} c_p \bar{T}) + \frac{\partial}{\partial z}(\rho \bar{w} c_p \bar{T}) \\ = K \left(\frac{\partial^2 \bar{T}}{\partial x^2} + \frac{\partial^2 \bar{T}}{\partial y^2} + \frac{\partial^2 \bar{T}}{\partial z^2} \right) - \frac{\partial}{\partial x_i}(\rho c_p \bar{T} \bar{u}'_i) + q'' \end{aligned} \quad (1.1)$$

Momentum in x-direction

$$\frac{\partial}{\partial t}(\rho \bar{u}) + \frac{\partial}{\partial x}(\rho \bar{u} \bar{u}) + \frac{\partial}{\partial y}(\rho \bar{v} \bar{u}) + \frac{\partial}{\partial z}(\rho \bar{w} \bar{u}) = -\frac{\partial \bar{P}}{\partial x} + \mu \left(\frac{\partial^2 \bar{u}}{\partial x^2} + \frac{\partial^2 \bar{u}}{\partial y^2} + \frac{\partial^2 \bar{u}}{\partial z^2} \right) - \frac{\partial}{\partial x_i}(\rho \bar{u}' u'_i)$$

(1.2)

Momentum in y-direction

$$\begin{aligned} \frac{\partial}{\partial t}(\rho \bar{v}) + \frac{\partial}{\partial x}(\rho \bar{u} \bar{v}) + \frac{\partial}{\partial y}(\rho \bar{v} \bar{v}) + \frac{\partial}{\partial z}(\rho \bar{w} \bar{v}) \\ = -\frac{\partial \bar{P}}{\partial y} + \mu \left(\frac{\partial^2 \bar{v}}{\partial x^2} + \frac{\partial^2 \bar{v}}{\partial y^2} + \frac{\partial^2 \bar{v}}{\partial z^2} \right) - \frac{\partial}{\partial x_i}(\rho \bar{v}' u'_i) - \rho g \beta (\bar{T}_\infty - \bar{T}) \end{aligned} \quad (1.3)$$

Momentum in z-direction

$$\frac{\partial}{\partial t}(\rho\bar{w}) + \frac{\partial}{\partial x}(\rho\bar{uw}) + \frac{\partial}{\partial y}(\rho\bar{vw}) + \frac{\partial}{\partial z}(\rho\bar{ww}) = -\frac{\partial\bar{P}}{\partial z} + \mu\left(\frac{\partial^2\bar{w}}{\partial x^2} + \frac{\partial^2\bar{w}}{\partial y^2} + \frac{\partial^2\bar{w}}{\partial z^2}\right) - \frac{\partial}{\partial x_i}(\rho\overline{w'u'_i})$$

(1.4)

Continuity

$$\frac{\partial}{\partial x}(\rho u) + \frac{\partial}{\partial y}(\rho v) + \frac{\partial}{\partial z}(\rho w) = 0$$

(1.5)

The momentum equations have the term $-\frac{\partial}{\partial x_i}(\rho\overline{u'_j u'_i})$ given in compact tensor notation. These terms represent the effect that turbulent motion has on the time-mean quantities known as Reynold's stresses which are high frequency fluctuating velocity components. The new terms in the energy equation $(-\frac{\partial}{\partial x_i}(\rho c_p \overline{T'u'_i}))$ represent the turbulent heat fluxes which are the fluctuating components of the temperature and velocity.

The eddy-viscosity concept proposed by Boussinesq can then be applied to the motion equations. The additional turbulent stresses are assumed to be proportional to the mean-velocity gradients. The stresses in tensor notation can be related as follows.

$$\overline{u'_j u'_i} = \frac{\mu_t}{\rho} \left(\frac{\partial \bar{u}_j}{\partial x_i} + \frac{\partial \bar{u}_i}{\partial x_j} \right) - \frac{2}{3} k \delta_{ji}$$

(1.6)

where μ_t is the eddy viscosity, k is the kinetic energy and δ_{ji} is the Kronecker delta. This approach is used in both the k-epsilon and k-omega models. The advantage being that computational costs are relatively low because of the computational power needed to calculate the turbulent viscosity. Also, the turbulent heat fluxes are assumed to be proportional to the mean temperature gradients and are again expressed in tensor notation.

$$-\rho c_p \overline{T' u_i'} = c_p \Gamma \frac{\partial \bar{T}}{\partial x_j}$$

(1.7)

where Γ is the turbulent diffusivity of heat. Both the eddy viscosity and the turbulent diffusivity of heat are properties of the flow, not the fluid. In order to relate these two quantities together, the turbulent Prandtl number is introduced. It can be assumed constant

as experiments have shown that this ratio does not vary in flows or between flows even though μ_t and Γ do.

$$\sigma_t = \frac{\mu_t}{\Gamma} \quad (1.8)$$

By substituting equations 1.6, 1.7 and 1.8 into the equations of motion (equations 1.1 to 1.5) the fluctuating quantities are removed as eddy viscosity and mean quantity gradients describe the turbulent diffusion and the equations of motion are represented as follows.

Energy

$$\begin{aligned} \frac{\partial}{\partial t}(\rho c_p \bar{T}) + \frac{\partial}{\partial x}(\rho \bar{u} c_p \bar{T}) + \frac{\partial}{\partial y}(\rho \bar{v} c_p \bar{T}) + \frac{\partial}{\partial z}(\rho \bar{w} c_p \bar{T}) \\ = K \left(\frac{\partial^2 \bar{T}}{\partial x^2} + \frac{\partial^2 \bar{T}}{\partial y^2} + \frac{\partial^2 \bar{T}}{\partial z^2} \right) + \frac{\partial}{\partial x_i} \left(\frac{\partial \bar{T}}{\partial x_i} \frac{c_p \mu_t}{\sigma_t} \right) + q''' \end{aligned} \quad (1.9)$$

Momentum in x-direction

$$\frac{\partial}{\partial t}(\rho \bar{u}) + \frac{\partial}{\partial x}(\rho \bar{u} \bar{u}) + \frac{\partial}{\partial y}(\rho \bar{v} \bar{u}) + \frac{\partial}{\partial z}(\rho \bar{w} \bar{u}) = -\frac{\partial \bar{P}}{\partial x} + (\mu + \mu_t) \left(\frac{\partial^2 \bar{u}}{\partial x^2} + \frac{\partial^2 \bar{u}}{\partial y^2} + \frac{\partial^2 \bar{u}}{\partial z^2} \right) \quad (1.10)$$

Momentum in y-direction

$$\frac{\partial}{\partial t}(\rho\bar{v}) + \frac{\partial}{\partial x}(\rho\bar{u}\bar{v}) + \frac{\partial}{\partial y}(\rho\bar{v}\bar{v}) + \frac{\partial}{\partial z}(\rho\bar{w}\bar{v})$$

(1.11)

$$= -\frac{\partial\bar{P}}{\partial y} + (\mu + \mu_t) \left(\frac{\partial^2\bar{v}}{\partial x^2} + \frac{\partial^2\bar{v}}{\partial y^2} + \frac{\partial^2\bar{v}}{\partial z^2} \right) - \rho g \beta (\bar{T}_\infty - \bar{T})$$

Momentum in z-direction

$$\frac{\partial}{\partial t}(\rho\bar{w}) + \frac{\partial}{\partial x}(\rho\bar{u}\bar{w}) + \frac{\partial}{\partial y}(\rho\bar{v}\bar{w}) + \frac{\partial}{\partial z}(\rho\bar{w}\bar{w}) = -\frac{\partial\bar{P}}{\partial z} + (\mu + \mu_t) \left(\frac{\partial^2\bar{w}}{\partial x^2} + \frac{\partial^2\bar{w}}{\partial y^2} + \frac{\partial^2\bar{w}}{\partial z^2} \right) \quad (1.12)$$

Continuity

$$\frac{\partial}{\partial x}(\rho\bar{u}) + \frac{\partial}{\partial y}(\rho\bar{v}) + \frac{\partial}{\partial z}(\rho\bar{w}) = 0$$

(1.13)

This form of the equations differs from the original instantaneous equations due only to the momentum and heat diffusion coefficients. The new terms in the momentum and energy equations represent the influence of turbulence on the time-mean quantities. The following sections describe the turbulence models that will be tested in order to determine which model gives the best results for large atrium flow, specifically the case described at the beginning of this section.

A.1.1 k-ε Turbulence Model

The k-ε model has become one of the most widely used turbulence models as it provides robustness, economy and reasonable accuracy for a wide range of turbulent flows [Malalasekera]. Improvements have been made to the standard model which improves its performance and two variants are available in Fluent; the RNG (renormalization group) model and the realizable model. The standard, RNG, and realizable models have similar form with transport equations for k and ε. The two

transport equations independently solve for the turbulent velocity and length scales. The main differences between the three models are as follows;

- The turbulent Prandtl Numbers governing the turbulent diffusion of k and ε
- The generation and destruction terms in the equation for ε
- The method of calculating turbulent viscosity

A.1.1.1 Standard k-Epsilon Turbulence Model

Fluent User's manual [] reveals that this model was initially proposed by Launder and Spalding (1972). As mentioned in Fluent User's manual [], for this model the transport equation for k is derived from the exact equation, but the transport for ε was obtained using physical reasoning and is, therefore, similar to the mathematically derived transport equation of k , but is not exact. The turbulent kinetic energy k , and its rate of dissipation ε , for this model are obtained by the following equations.

$$\frac{\partial}{\partial t}(\rho k) + \frac{\partial}{\partial x_i}(\rho k u_i) = \frac{\partial}{\partial x_j} \left[\left(\mu + \frac{\mu_t}{\sigma_k} \right) \frac{\partial k}{\partial x_j} \right] + G_k + G_b - \rho \varepsilon - Y_M + S_K$$

(1.14)

$$\frac{\partial}{\partial t}(\rho \varepsilon) + \frac{\partial}{\partial x_i}(\rho \varepsilon u_i) = \frac{\partial}{\partial x_j} \left[\left(\mu + \frac{\mu_t}{\sigma_\varepsilon} \right) \frac{\partial \varepsilon}{\partial x_j} \right] + C_{1\varepsilon} \frac{\varepsilon}{k} (G_k + C_{3\varepsilon} G_b) - C_{2\varepsilon} \rho \frac{\varepsilon^2}{k} + S_\varepsilon$$

(1.15)

where G_k represents the generation of turbulent kinetic energy that arises due to mean velocity gradients, G_b is the generation of turbulent kinetic energy that arises due to buoyancy, and Y_M represents the fluctuating dilation in compressible turbulence that contributes to the overall dissipation rate. S_ε and S_k are source terms defined by the user. $C_{1\varepsilon}$, $C_{2\varepsilon}$ and C_μ are constants that have been determined experimentally and are taken to have the following values;

$$C_{1\varepsilon}=1.44, C_{2\varepsilon} = 1.92 \text{ and } C_\mu = 0.09$$

σ_k and σ_s are turbulent Prandtl numbers for the turbulent kinetic energy and its dissipation rate. These have also been derived experimentally and are defined as follows.

$$\sigma_k = 1.0, \sigma_s = 1.3$$

The turbulent (or eddy) viscosity at each point is related to the local values of turbulent kinetic energy and its dissipation rate by;

$$\mu_t = \rho C_\mu \frac{k^2}{\varepsilon}$$

(1.16)

where C_μ is constant and defined above. The term for the production of turbulent kinetic energy G_k is common in many of the turbulence models studied and is defined as

$$G_k = -\overline{\rho u'_i u'_j} \frac{\partial u_j}{\partial x_i}$$

(1.17)

The modulus of mean rate-of-strain tensor, S is defined as

$$S = \sqrt{2S_{ij}S_{ij}}$$

(1.18)

The generation of turbulent kinetic energy that arises due to buoyancy, G_b is defined as follows

$$G_b = \beta g_i \frac{\mu_t}{Pr_t} \frac{\partial T}{\partial x_i}$$

(1.19)

As the present study uses relatively low velocities, the dilation dissipation term, Y_M which accounts for turbulence from compressibility effects is defined as

$$Y_M = 2\rho\varepsilon M_i^2$$

(1.20)

A.1.1.2 RNG k-Epsilon Turbulence Model

Similar to the standard k-epsilon model, the RNG model was derived from the instantaneous Navier Stokes equations, except it uses a technique called renormalization group theory described by Yakhot and Orszag (1986) as mentioned in Fluent User's manual []. This derivation produces a model with different constants to those used in the standard k-epsilon model and also adds new terms to the transport equations for the turbulent kinetic energy and its dissipation. The effect of swirl is also accounted for in the RNG model enhancing the accuracy of swirling flows. An analytical formula for turbulent Prandtl - numbers is provided in this model while the standard model relies on user-specific constant values. Finally, assuming appropriate treatment of the near wall region, the RNG model uses an analytically derived differential formula for the effective turbulent viscosity which accounts for low Reynolds number flows. The RNG k-Epsilon model is therefore more accurate and more reliable than the standard k-Epsilon model for a wider range of flows. As a result from these differences, the transport equations appear as follows.

$$\frac{\partial}{\partial t}(\rho k) + \frac{\partial}{\partial x_i}(\rho k u_i) = \frac{\partial}{\partial x_j} \left[\alpha_k \mu_{eff} \frac{\partial k}{\partial x_j} \right] + G_k + G_b - \rho \varepsilon - Y_M + S_K$$

(1.21)

where G_k represents the generation of turbulent kinetic energy that arises due to mean velocity gradients, G_b is generation of turbulent kinetic energy that arises due to buoyancy, and Y_M represents the fluctuating dilation in compressible turbulence that contributes to the overall dissipation rate. S_ε and S_k are source terms defined by the user. α_k and α_ε are inverse effective Prandtl numbers for the turbulent kinetic energy and its dissipation. The RNG theory uses a scale elimination procedure that defines the effective viscosity given in the following equation.

$$d \left(\frac{\rho^2 k}{\sqrt{\varepsilon \mu}} \right) = 1.72 \frac{\hat{\nu}}{\sqrt{\hat{\nu}^3 - 1 + C_\nu}} d\hat{\nu}$$

(1.22)

where $\hat{\nu} = \mu_{eff} / \mu$ and C_ν is a constant equal approximately to 100. This equation incorporates the ability to accurately define how the effective turbulent transport

varies with effective Reynolds number to obtain more accurate results for low-Re flows and near-wall flows. For high Reynolds numbers, the effective viscosity is defined by the following ratio;

$$\mu_t = \rho C_\mu \frac{k^2}{\varepsilon}$$

(1.23)

Although this is similar to the turbulent viscosity of the standard model, the constant C_μ is derived using the RNG theory and found to be 0.0845 which is very close to the value used

in the standard model (i.e., 0.09). $C_{1\varepsilon}$ and $C_{2\varepsilon}$ are constants that have been derived analytically by the RNG theory and are defined as follows.

$$C_{1\varepsilon}=1.42, C_{2\varepsilon}=1.68$$

A.1.1.3 Realizable k-Epsilon Turbulence Model

The Realizable model by Shih (1995) is the most recently developed of the three k-Epsilon variations and features two main differences from the standard k-Epsilon model. Fluent User's manual reveals that this model uses a new equation for the turbulent viscosity and the dissipation rate transport equation has been derived from the equation for the transport of the mean-square vorticity fluctuation. The form of the eddy viscosity (turbulent) equations is based on the realizability constraints; the positivity of normal Reynolds stresses and Schwarz' inequality for turbulent shear stresses (i.e., certain mathematical constraints on the normal stresses are satisfied). This is not satisfied by either the standard or the RNG k-epsilon models which makes the realizable model more precise than both models at predicting flows such as separated flows and flows with complex secondary flow features.

The term "realizable" means that the model satisfies certain mathematical constraints on the Reynolds stresses, consistent with the physics of turbulent flows. Neither the standard k- ε model nor the RNG k- ε model is realizable.

An immediate benefit of the realizable k- ε model is that it more accurately predicts the spreading rate of both planar and round jets. It is also likely to provide superior

performance for flows involving rotation, boundary layers under strong adverse pressure gradients, separation and recirculation.

In terms of the improved changes by Shih (1995), the transport equations become:

$$\frac{\partial}{\partial t}(\rho k) + \frac{\partial}{\partial x_j}(\rho k u_j) = \frac{\partial}{\partial x_j} \left[\left(\mu + \frac{\mu_t}{\sigma_k} \right) \frac{\partial k}{\partial x_j} \right] + G_k + G_b - \rho \varepsilon - Y_M + S_K \quad (1.24)$$

$$\begin{aligned} \frac{\partial}{\partial t}(\rho \varepsilon) + \frac{\partial}{\partial x_j}(\rho \varepsilon u_j) \\ = \frac{\partial}{\partial x_j} \left[\left(\mu + \frac{\mu_t}{\sigma_\varepsilon} \right) \frac{\partial \varepsilon}{\partial x_j} \right] + \rho C_1 S \varepsilon - \rho C_2 \frac{\varepsilon^2}{k + \sqrt{\nu \varepsilon}} + C_{1\varepsilon} \frac{\varepsilon}{k} C_{3\varepsilon} G_b + S_\varepsilon \end{aligned} \quad (1.25)$$

where G_k represents the generation of turbulent kinetic energy that arises due to mean velocity gradients, G_b is generation of turbulent kinetic energy that arises due to buoyancy, and Y_M represents the fluctuating dilation in compressible turbulence that contributes to the overall dissipation rate. S_ε and S_k are source terms defined by the user. α_k and α_ε are the turbulent Prandtl numbers for the turbulent kinetic energy and its dissipation. Similar to the previous variations of the k-Epsilon models, the turbulent viscosity is determined by the formula given below; however it produces different results as C_μ is not constant.

$$\mu_t = \rho C_\mu \frac{k^2}{\varepsilon} \quad (1.26)$$

where C_μ is computed from

$$C_\mu = \frac{1}{A_0 + A_S \frac{kU^*}{\varepsilon}} \quad (1.27)$$

where

$$U^* = \sqrt{S_{ij}S_{ij} + \tilde{\Omega}_{ij}\tilde{\Omega}_{ij}} \quad \text{and} \quad \tilde{\Omega}_{ij} = \overline{\Omega_{ij}} - \varepsilon_{ijk}\omega_k - 2\varepsilon_{ijk}\omega_k$$

In the above equation, $\overline{\Omega_{ij}}$ is the mean rate of rotation tensor viewed in a rotating reference frame with angular velocity ω_k . The constants A_0 and A_S are defined as;

$$A_0 = 4.04, \quad A_S = \sqrt{6} \cos \phi$$

where

$$\phi = \frac{1}{3} \cos^{-1} \left(\sqrt{6} \frac{S_{ij}S_{jk}S_{ki}}{\tilde{S}^3} \right), \quad \tilde{S} = \sqrt{S_{ij}S_{ij}}, \quad S_{ij} = \frac{1}{2} \left(\frac{\partial u_j}{\partial x_i} + \frac{\partial u_i}{\partial x_j} \right)$$

It has been shown that C_μ is a function of the mean strain and rotational rates, the angular velocity of the rotating system, and the turbulent kinetic energy and its dissipation rate. The standard value of $C_\mu = 0.09$ is found to be the solution of equation 1.27 for an inertial sub layer in the equilibrium boundary layer. The constants $C_{1\varepsilon}$, C_2 , σ_k and σ_ε have been determined by Shih (1995) and are defined as follows.

$$C_{1\varepsilon}=1.44, \quad C_2=1.9, \quad \sigma_k=1.0, \quad \sigma_\varepsilon = 1.2$$

APPENDIX A.2

DESIGN OF EATHE

Preliminary design of EATHE use basic heat transfer and fluid flow equations. The design parameters of EATHE are selected according to space conditioning. The mass flow rate and outlet temperature of ventilating air, which are the sizing parameters are the fixed for a specified requirement. Now input parameter and variables are required to identify which affect the effectiveness of EATHE system.

The inlet air temperature and ground temperature vary with climate condition. The soil temperature at a depth of 3-4 meter is estimated as mean annual average temperature at particular location. Once the design output is fixed then we directly relate our governing equations to estimate length of tube, pressure drop across one particular tube and effectiveness.

A.1.1 Dimensions of EATHE

The geometric parameters of an EATHE include the tube diameter (D), Tube length (L) and number of tubes in parallel (n) in the heat exchanger. First we select arbitrary size (D) of tube and then with the help of known mass flow rate the number of parallel tube are calculated. We have to select optimum combination of size and number of tubes to meet EATHE performance. For a tube diameter (D), air density (ρ) air flow velocity (v) and number of parallel tubes (n); the mass flow rate of air through a tube, \dot{m} is given by:

$$\dot{m} = \frac{\frac{\pi D^2 \rho v}{4}}{n} \quad (1)$$

These parameters are selected in such a way that the boundary conditions and the EATHE performance are met.

A.1.2 Earth ground temperature

Earth surface temperature varies with climate condition at particular location and also varies from morning to evening. After selecting the location, fluctuation in ground temperature can be reduced by increasing depth. At 3-4 m depth of ground temperature is nearly constant which is called earth un-disturbed temperature. The

temperature at depth z and time t can be calculated for homogeneous soil of constant thermal diffusivity.

$$T_{z,t} = T_m - Ae^{\left[-z\left(\frac{\pi}{365\alpha}\right)^{\frac{1}{2}}\right]} \cos\left[\frac{2\pi}{365}\left\{t-t_0-\frac{z}{2}\left(\frac{365}{\pi\alpha}\right)^{\frac{1}{2}}\right\}\right] \quad (2)$$

Where $T_{z,t}$ is the ground temperature at time t (s) and depth z (m), T_m is the average soil surface temperature ($^{\circ}\text{C}$), A is the amplitude, α is the soil thermal diffusivity (m^2/s), t is the time elapsed from beginning of the calendar year (day) and t_0 is the phase constant of soil surface (s). Generally earth ground temperature (EUT) is taken as mean annual average air temperature at specified location.

A.1.3 Assumptions

To simplify the design equations following assumptions are made.

1. Temperature of surrounding soil of tube is constant (uniform temperature in axial direction)
2. Earth ground temperature (EUT) is constant along the length of tube.
3. Turbulent flow of air throughout the tube so that entrance length is small in the small size tube.
4. The surface temperature of the ground is taken as ambient air temperature, which is equal to inlet air temperature.
5. Thermal resistance of pipe is negligible.
6. The temperature on the surface of tube taken as uniform in axial direction and which is equal to earth's undisturbed temperature.
7. Uniform cross-section of tube with smooth surface at inner side.
8. Thermo-physical properties (density, viscosity, thermal conductivity and specific heat capacity etc.) of air and soil are constant.

A.1.4 Heat transfer

If the output of EATHE system is fixed, inlet conditions are known then heat transfer can be calculated using log mean temperature difference (LMTD) or number of

transfer units (NTU) or by calculating over all heat transfer coefficient. In this paper we used NTU method because of its simplicity.

In the earth air tunnel heat exchanger, air is the transportation medium. The heat is being released or absorbed by the air by heat transfer process between air and underground soil. Heat transfer between air and the tube wall by convection and from tube wall to the surrounding soil by conduction. If the contact of the tube wall with the earth is assumed to be perfect and the conductivity of the soil is taken to be very high compared to the surface resistance, then the wall temperature at the inside of the tube can be assumed to be constant.

The total heat transfer to the air flowing through a buried tube is given by:

$$Q_t = \dot{m}C_{p,a} (T_{out} - T_{in}) \quad (3)$$

Where \dot{m} is the mass flow rate of air (kg/s), $C_{p,a}$ is the specific heat of air (J/kg-K), T_{out} is the temperature of air at outlet of EATHE tube ($^{\circ}$ C), and T_{in} is the temperature of air at inlet of EATHE tube($^{\circ}$ C).

Due to convection between tube wall and the air, the heat transfer can also be given by:

$$Q_t = h_c A \Delta Tlm \quad (4)$$

Where h_c ; the convective heat transfer coefficient from inner side to outer side of tube and A is the internal surface area of the tube.

Over all heat transfer coefficient per unit length from air to soil is given as:

$$U_t = \left(\frac{1}{h_c} + \frac{1}{2\pi k_t} \log \frac{r_o}{r_i} \right)^{-1} \quad (5)$$

$$Q_t = U_t A \Delta Tlm \quad (6)$$

Where k_t ; the thermal conductivity of tube, r_o is the outer radius of tube, r_i is the inner radius of tube. In this equation we assume that thermal resistance of tube is negligible. h_c can be calculated with the help of Nusselt number.

$$h_c = \frac{NuK}{D}$$

Where K ; the thermal conductivity of air, N_u is Nusselt number and D is the hydraulic diameter of cross section. The value of Nusselt number is given by:

$$N_u = \frac{f/8(R_e - 1000)P_r}{1 + 12.7\sqrt{f/8} (P_r^{2/3} - 1)} \quad \text{for turbulent flow } R_e > 2300 \quad (7)$$

$$N_u = 3.66 \quad \text{for laminar flow } R_e < 2300 \quad (8)$$

Where R_e ; the Reynolds number, P_r is Prandtl number, and f is the friction factor for smooth surface.

$$f = (1.82 \log R_e - 1.64)^{-2} \quad 2300 \leq R_e < 5 \times 10^6 \text{ and } 0.5 < P_r < 10^6$$

The Reynolds number is calculated using the average air flow velocity (v) and diameter of tube (D):

$$R_e = \frac{\rho v D}{\mu}$$

The Prandtl number is defined as: $P_r = \frac{\mu c_p}{K}$ where c_p is the specific heat of air.

Once h_c or U_t is calculated the outlet air temperature of EATHE system can be estimated as a function of tube wall temperature and inlet air temperature using equation (3) and (4)

$$T_{out} = T_{wall} + (T_{in} - T_{wall})e^{-(hA/\dot{m}C_{p,a})} \quad (9)$$

And using equation (1) and (3)

$$T_{out} = T_{wall} + (T_{in} - T_{wall})e^{-(U_t A/\dot{m}C_{p,a})} \quad (10)$$

Non dimensional heat transfer unit (NTU) is defined as:

$$NTU = \frac{h_c A}{\dot{m}C_{p,a}} = U_t A/\dot{m}C_{p,a} \quad (11)$$

Here area is defined $A = 2\pi r_i l$.

The effectiveness of EATHE system is defined as:

$$\epsilon = \frac{(T_{out}-T_{in})}{(T_{wall}-T_{in})} = 1 - e^{-NTU}$$

(12)

A.1.5 Design equations

Development of design equations are derived from above relations. For estimating the length of tube and pressure drop across the tube we are known to the value of total volume flow rate, size of tube, depth at which tubes are placed and number of parallel tubes.

Pressure drop across the can be estimated without considering tube bend effect.

$$\Delta P = \rho f \frac{v^2}{4r_i} L$$

(13)

Where $f = \frac{64}{Re}$ if $Re < 2300$;

And $f = (1.82 \log Re - 1.64)^{-2}$ if $Re > 2300$

Now air fan power (AFP) is given as follow for total pressure drop (ΔP) and total volume flow rate of air (V).

$$AFP = V \Delta P$$

(14)

The value of NTU as follow:

$$NTU = -\ln(1 - \epsilon)$$

(15)

Now the required length of tube for derived value of NTU using relation.

$$L = \frac{\dot{m} C_{p,a} NTU}{h_c}$$

(16)

Both NTU and ΔP are proportional to the length of the tube and we can use NTU/L and $\Delta P/L$ as the main performance characteristics to determine the desired length of tube for specified effectiveness.

A.1.6 HX design sheet (Mathematical analysis)

In the HX design sheet the effectiveness of EATHE is fixed according to set of input parameter and fixed output parameter. With the help of input of tube size (D), inlet temperature, volume flow rate (V), number of parallel tube (n), mean annual average air temperature and fixed output temperature the value of NTU is estimated. For the

determining of length of tube for a desired NTU parameter we used design calculations. The mean temperature input in Celsius and selected PVC material of tube having thermal conductivity (k_t) equal to 0.19 W/MK. We select surface roughness ϵ for different tube material using ASHRAE STANDARD 2009. The main output of design sheet is length of tube (m), pressure drop across the tube, NTU, U_t , h_c and effectiveness.

$$\frac{m}{\rho} = 0.0945 \text{ m}^3/\text{sec}, \text{ Diameter of Tube (D)} = 0.10 \text{ m}, \text{ Dynamic Viscosity of air } (\mu) = 1.804\text{E-}05 \text{ (kg/m-s)};$$

TABLE: A.2.1. Different design parameters with varying flow velocities

PARAMETERS	$V_a = 3 \text{ m/sec}$	$V_a = 4\text{m/sec}$	$V_a = 5\text{m/sec}$
Re	20371.39	27,161.85	33,952.316
Pr	0.715	0.715	0.715
F	0.0255	0.0241	0.02291
Nu	52.63	65.49	76.51
h_c	13.3	16.571	19.359
NTU	2.16	2.699	3.153
ϵ	0.884	0.932	0.957
L (m)	18.89	18.83	18.82
ΔP (pa)	2.65	4.44	6.6

TABLE: A.2.2. Thermo-physical properties of materials used in calculations

Parameter	Material		
	Air	Soil	PVC
Density (kg m^{-3})	1.225	2050	1380
Specific heat capacity ($\text{J kg}^{-1} \text{K}^{-1}$)	1006	1840	900
Thermal conductivity ($\text{W m}^{-1} \text{K}^{-1}$)	0.0242	0.52	0.19

APPENDIX A.3**SIMULATION DATA OF DRY AND WETTED EATHE****Table A.3.1: Hourly variations in air temperature along the length of pipe for dry tunnel**

Length of pipe (m)	Temperature of air along the length of pipe ($^{\circ}$ K)					
	After 1 hour		After 6 hours		After 11 hours	
	Experiment (16/6/2016)	Simulation	Experiment (16/6/2016)	Simulation	Experiment (16/6/2016)	Simulation
Inlet	313.0	313.0	318.5	318.5	311.6	311.6
5	310.5	310.5	316.2	315.6	310.1	309.9
10	309.3	307.2	314.1	312.4	309.1	308.1
20	307.1	303.6	310.6	307.7	308.3	305.3
30	306.6	301.7	307.5	304.7	307.1	303.4
40	305.5	300.8	305.5	302.8	305.4	302.2
60	304.2	300.9	304.2	301.0	304.2	300.8

Table A.3.2: Hourly variations in air temperature along the length of pipe for wet tunnel (5% wetness)

Length of pipe (m)	Temperature of air along the length of pipe ($^{\circ}$ K)					
	After 1 hour		After 6 hours		After 11 hours	
	Experiment (16/6/2016)	Simulation	Experiment (16/6/2016)	Simulation	Experiment (16/6/2016)	Simulation
Inlet	312.2	312.2	318.5	318.5	311.6	311.6
5	310.5	309.8	314.3	315.1	309.9	309.7
10	309.2	306.7	311.6	311.5	308.1	307.6
20	307.2	303.1	307.7	306.6	306.2	304.6
30	304.5	301.4	304.5	303.7	304.3	302.7
40	304.2	300.7	304.2	302.1	304.1	301.6
60	303.8	300.2	303.8	300.6	303.8	300.5

Table A.3.3: Hourly variations in air temperature along the length of pipe for wet tunnel (10% wetness)

Length of pipe (m)	Temperature of air along the length of pipe ($^{\circ}$ K)					
	After 1 hour		After 6 hours		After 11 hours	
	Experiment (20/6/2016)	Simulation	Experiment (20/6/2016)	Simulation	Experiment (20/6/2016)	Simulation
Inlet	311.9	311.9	318.5	318.5	312.1	312.1
5	310.5	307.4	315.2	312.5	310.1	308.4
10	308.2	303.9	312.1	307.4	308.1	305.2
20	306.7	301.2	307.5	302.6	306.7	301.9
30	304.5	300.4	304.3	300.9	304.4	300.7
40	304.1	300.2	303.9	300.4	304.1	300.3
60	303.7	300.1	303.6	300.1	303.6	300.1

Table A.3.4: Hourly variations in air temperature along the length of pipe for wet tunnel (15% wetness)

Length of pipe (m)	Temperature of air along the length of pipe ($^{\circ}$ K)					
	After 1 hour		After 6 hours		After 11 hours	
	Experiment (20/6/2016)	Simulation	Experiment (20/6/2016)	Simulation	Experiment (20/6/2016)	Simulation
Inlet	311.7	311.7	318.5	318.5	311.6	311.6
5	310.1	307.1	314.3	312.1	309.9	307.8
10	308.4	303.7	311.1	306.9	308.1	304.8
20	306.2	301.0	306.5	302.3	306.7	301.6
30	304.4	300.3	304.3	300.9	304.5	300.5
40	304.1	300.1	303.9	300.2	304.1	300.2
60	303.8	300.1	303.6	300.1	303.8	300.1